Benzothiopyranoindole- and pyridothiopyranoindole-based antiproliferative agents targeting topoisomerases.

Silvia Salerno,[a,‡] Valeria La Pietra,[b,‡] Mariafrancesca Hyeraci,[c] Sabrina Taliani,[a,*] Marco Robello,[d] Elisabetta Barresi,[a] Ciro Milite,[e] Francesca Simorini,[a] Aída Nelly García-Argáez,[c,f] Luciana Marinelli,[b,*] Ettore Novellino,[b] Federico Da Settimo,[a] Anna Maria Marini,[a] Lisa Dalla Via.[c]

[a]Dipartimento di Farmacia, Università di Pisa, Via Bonanno 6, 56126 Pisa, Italy.

[b]Dipartimento di Farmacia, Università di Napoli "Federico II", Via D. Montesano 49, 80131 Napoli, Italy.

[c]Dipartimento di Scienze del Farmaco, Università di Padova, Via Marzolo 5, 35131 Padova, Italy.

[d]Synthetic Bioactive Molecules Section LBC, NIDDK, NIH, 8 Center Dr., 20982, Bethesda, Maryland, USA.

[e]Dipartimento di Farmacia, Università di Salerno, Via Giovanni Paolo II 132, 84084 Fisciano, Salerno, Italy.

[f]Fondazione per la Biologia e la Medicina della Rigenerazione T.E.S., Via Marzolo 13, 35131, Padova, Italy.

Abstract

New benzothiopyranoindoles (**5a-l**) and pyridothiopyranoindoles (**5m-t**), featuring different combinations of substituents (H, Cl, OCH_3) at R^2-R^4 positions and protonatable R^1-dialkylaminoalkyl chains, were synthesized and biologically assayed on three human tumor cell lines, showing significant antiproliferative activity (GI_{50} values spanning from 0.31 to 6.93 μM) and pro-apoptotic effect. Linear flow dichroism experiments indicate the ability of both chromophores to form a molecular complex with DNA, following an intercalative mode of binding. All compounds displayed a moderate ability to inhibit the relaxation activity of both topoisomerases I and II, reasonably correlated to their intercalative capacities. Cleavable assay performed with topoisomerase I revealed a significant poisoning effect for compounds **5g**, **5h**, **5s**, and **5t**. A theoretical model provided by hydrated docking calculations clarified the role of the R^1-R^4 substituents on the topoisomerase I poison activity, revealing a crucial role of the R^2-OCH_3 group.

Keywords: benzothiopyranoindoles, pyridothiopyranoindoles, antiproliferative activity, topoisomerases, topoisomerase I poisons.

Abbreviation: A-431, squamous carcinoma cell line; AD4, AutoDock (version 4.2); ADT, AutoDockTools; *m*-AMSA, *m*-amsacrine; CPT, camptothecin; HeLa, cervix adenocarcinoma cell line; GALS, genetic algorithm local search; LD, linear flow dichroism; MSTO-211H, biphasic mesothelioma cell line; Topo I, type I topoisomerase; Topo II, type II topoisomerase.

1. Introduction

A large percentage of the chemotherapeutic anticancer agents currently used belong to the category of DNA-intercalating small molecules [1,2]. Some of them are valuable drugs for the treatment of ovarian and breast cancers and acute leukemias, while many others are in different phases of clinical trials [3-5]. Characteristic structural features of intercalating agents include the presence of planar polyaromatic systems, which interact reversibly with DNA by insertion between base-pairs, and elicit structural modifications leading to functional changes of transcription and replication processes, culminating in cellular death [1,5].

Several DNA-intercalating agents are also able to affect topoisomerase catalytic activity, thus producing permanent DNA strand breaks [1,6-10]. In humans, type I topoisomerase (Topo I) and type II topoisomerase (Topo II), are nuclear enzymes essential to resolve topological problems that occur during DNA transcription, replication, and chromosome segregation [11-15]. Thus, the biological functions of topoisomerases are crucial for ensuring genomic integrity, and the ability to interfere with these enzymes or generate enzyme-mediated damage is an effective strategy for cancer therapy [16-18]. In particular, drugs that interfere with the catalytic cycle by trapping a covalent intermediate, the cleavage complex, are commonly referred as poisons, while those that suppress enzyme activity by other mechanisms are named catalytic inhibitors. In this regard, Topo I and Topo II poisons represent a significant class of anticancer agents, forming the basis of many multidrug chemotherapy protocols widely used in a broad spectrum of tumors [16,19-23].

Camptothecin (CPT, **1**) [24], topotecan **2**, and irinotecan **3** (Chart 1) represent the most important Topo I poisons [19]. Drugs targeting Topo II include both poisons, (etoposide, doxorubicin, *m*-amsacrine (*m*-AMSA) and mitoxantrone), and inhibitors (bisdioxopiperazines or novobiocin, merbarone and the anthracycline aclarubicin) [23].

The two FDA-approved water-soluble derivatives **2** and **3** derived from efforts to improve the toxicity profile and pharmacokinetics of **1**, and are currently used for the treatment of solid tumors, **2** (Chart 1) for ovarian and lung cancers, and **3** (Chart 1) mainly for colon cancer [22]. Despite their efficiency

in the clinic, current anticancer therapies with these CPT derivatives are limited by some important drawbacks, including the emergence of drug-resistance [19,20,25]. Consequently, significant investments have been expended and are currently being made, and several chemical classes of non-CPT Topo I poisons were developed as promising antitumor drugs [16,23].

As part of our research program, devoted to the identification of new antiproliferative agents, we studied several polyheterocyclic chromophores, structurally related to classes of DNA intercalating agents [26-29]. Among them, the benzothiopyranoindoles **4a-v** [30] (Chart 1) were extensively studied, leading to the identification of a number of derivatives showing an antiproliferative activity at low micromolar concentrations [30]. Furthermore, it was proven that the chromophore scaffold itself does not possess any significant antiproliferative effect, unless a basic side chain on the indole nitrogen atom is present. It was also demonstrated a significant intercalation ability, as well as the capacity to inhibit the relaxation of supercoiled plasmid DNA mediated by Topo II in a dose-dependent manner. Finally, for the most cytotoxic derivative **4e** (Chart 1, X=OCH_3, X'=H, R^1=$(CH_2)_2N(CH_3)_2$), a weak Topo II poisoning effect and the capacity to inhibit the Topo I-mediated DNA relaxation were also demonstrated [30].

The successful results obtained from the benzothiopyranoindoles **4a-v** (Chart 1) [30] prompted the synthesis of a library of new derivatives from this class (**5a-t**, Chart 1), in order to evaluate the effect of various structural modifications on antiproliferative activity. In particular, while maintaining the benzothiopyranoindole system, a methoxy group was inserted at the 3-position (R^3) of the chromophore and variously combined with an additional methoxy at the 2-position (R^2) and/or methoxy/chlorine substituent at the 7-position (R^4), allowing the obtainment of the novel compounds **5a-d** and **5g-l** (Scheme 1). In addition, to investigate the effect of a double substitution with chlorine at either 3- and 7-positions of the planar moiety, derivatives **5e-f** (Scheme 1) were also synthesized. Finally, a small library of pyridothiopyranoindole isosters **5m-t** (Scheme 1) were studied; in this case, the introduction into the chromophore of a protonatable nitrogen atom could provide an additional or alternative anchor point in the formation of the intercalation complex.

All derivatives have been then functionalized with dialkylaminoalkyl chains (R^1), considering the crucial role of these basic moieties for the biological activity. To this regard we decided to focus on the dimethylaminoethyl and diethylaminoethyl chains, as they characterized the most active compounds of series **4** (Chart 1) [30].

The ability of the new benzothiopyranoindole (**5a-l**) and pyridothiopyranoindole (**5m-t**) derivatives to exert an antiproliferative activity was evaluated by means of an inhibition growth assay on three human tumor cell lines: cervix adenocarcinoma (HeLa), epidermoid carcinoma (A-431) and biphasic mesothelioma (MSTO-211H). Linear flow dichroism (LD) experiments were performed to assess the occurrence of a molecular complex with DNA. In addition, the ability of the compounds to interfere with the catalytic activity of both Topo I and Topo II was evaluated.

Finally, a molecular modeling study was carried out to shed light on the interaction between Topo I covalently bound to DNA and our poisons. Molecular determinants of our compounds regarding the poison property towards Topo I have also been discussed.

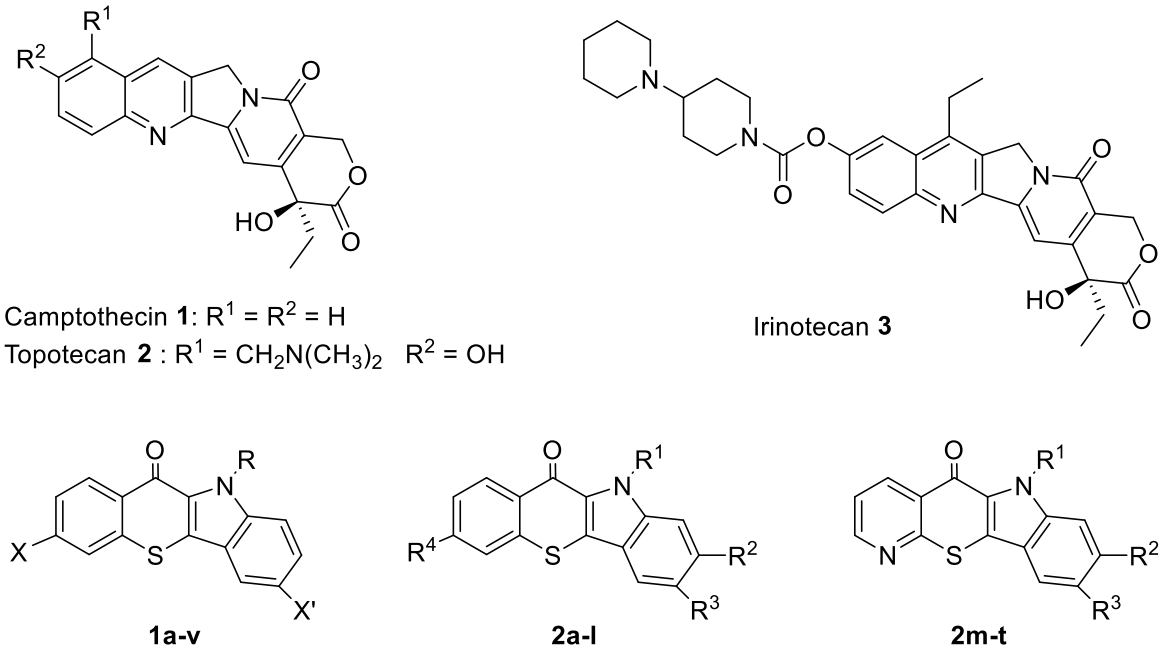

Chart 1. Structures of known (**1-4**) and newly synthesized (**5**) compounds targeting Topoisomerases.

2. Results and discussion

2.1 Chemistry

The preparation of the 11-dialkylaminoalkyl-2,3,7-substituted-benzothiopyrano[3,2-*b*]indol-10(11*H*)-ones **5a-l**, and 6-dialkylaminoalkyl-8,9-substituted-pyrido[3',2':5,6]thiopyrano[3,2-*b*]indol-5(6*H*)-ones **5m-t** was performed following the synthetic procedure outlined in Scheme 1.

The key starting 3-hydroxymethylenebenzothiopyranone derivatives **6a-c** [30,31] and 2,3-dihydro-3-(hydroxymethylene)-4*H*-thiopyran[2,3-*b*]pyridin-4-one **6d** [27], containing a methine active group, gave the desired 3-phenylhydrazono intermediates **8a-j**, in particularly good yields, by coupling with the appropriate substituted diazonium salt, using the Japp-Klingemann reaction [30,27,32]. Compounds **8a-j** were directly converted to the desired indoles **9a-j** with good to high yields using the Fischer cyclization, by refluxing in ethanolic hydrogen chloride solution. All the structures proposed for compounds **9a-j** agreed with ^{1}H-NMR spectral data, in which an interesting feature was the low-field signal (δ≈12 ppm), which was exchangeable with D_2O and was assigned to the proton of the indole NH group. The target 11-*N*-dialkylaminoalkyl-benzo substituted derivatives **5a-l** and 6-dialkylaminoalkyl-pyrido derivatives **5m-t** were obtained by reaction of compounds **9a-j** with the appropriate commercially available dialkylaminoalkylchloride hydrochlorides in anhydrous DMF solution, in the presence of sodium hydride. In the alkylated derivatives **5a-t** ^{1}H-NMR spectra, the exchangeable singlet, observed around 12 ppm as characteristic of the indole NH proton of compounds **9a-j**, disappears. In addition, the ^{1}H-NMR spectra of the alkylated derivatives **5a-t** clearly show the aliphatic protons signals, whose multiplicity is in agreement with the structures of the side chains introduced on the system.

Scheme 1

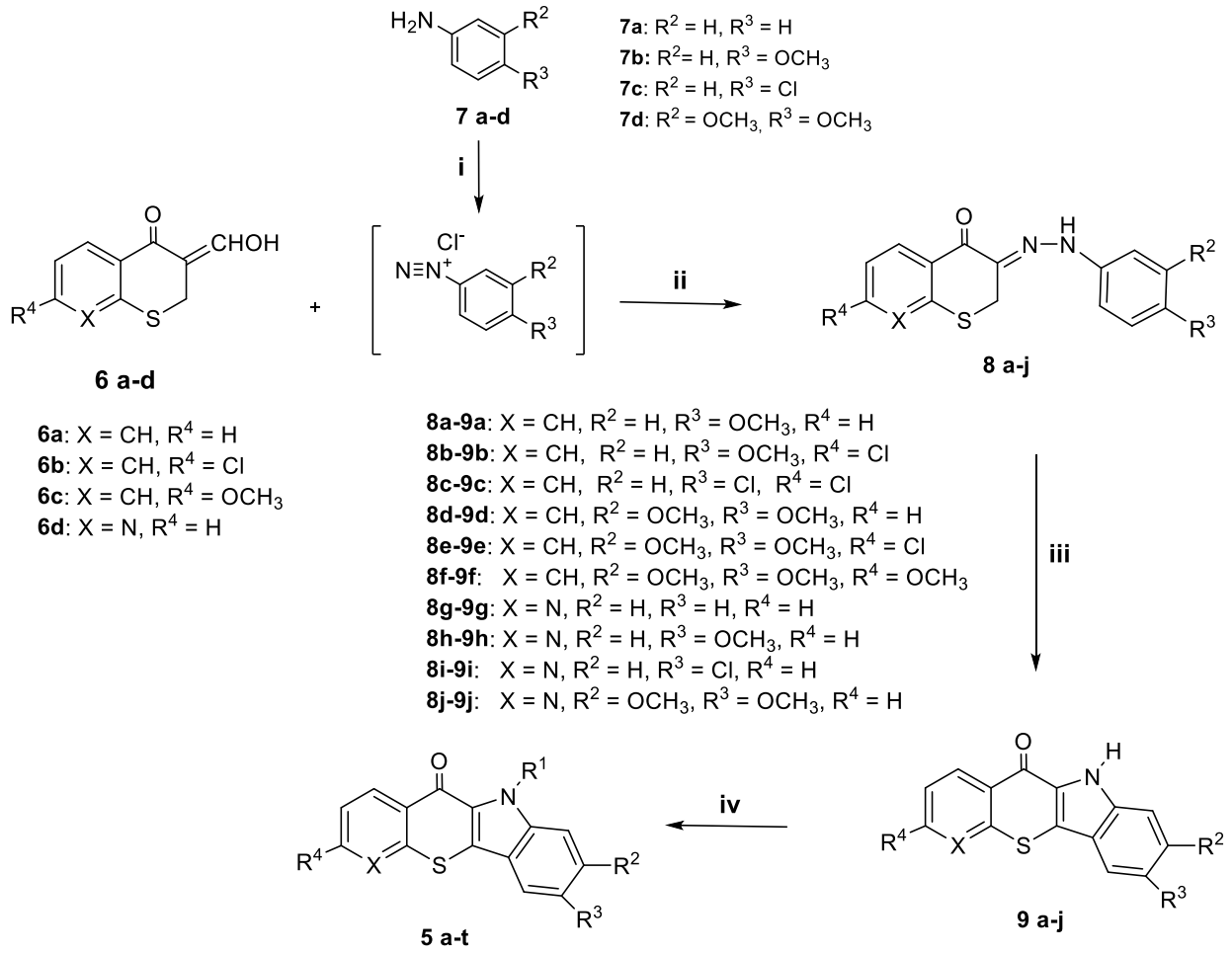

5a: X = CH, $R^1 = (CH_2)_2(CH_3)_2$, R^2 = H, $R^3 = OCH_3$, R^4 = H
5b: X = CH, $R^1 = (CH_2)_2(C_2H_5)_2$, R^2 = H, $R^3 = OCH_3$, R^4 = H
5c: X = CH, $R^1 = (CH_2)_2(CH_3)_2$, R^2 = H, $R^3 = OCH_3$, R^4 = Cl
5d: X = CH, $R^1 = (CH_2)_2(C_2H_5)_2$, R^2 = H, $R^3 = OCH_3$, R^4 = Cl
5e: X = CH, $R^1 = (CH_2)_2(CH_3)_2$, R^2 = H, R^3 = Cl, R^4 = Cl
5f: X = CH, $R^1 = (CH_2)_2(C_2H_5)_2$, R^2 = H, R^3 = Cl, R^4 = Cl
5g: X = CH, $R^1 = (CH_2)_2(CH_3)_2$, $R^2 = OCH_3$, $R^3 = OCH_3$, R^4 = H
5h: X = CH, $R^1 = (CH_2)_2(C_2H_5)_2$, $R^2 = OCH_3$, $R^3 = OCH_3$, R^4 = H
5i: X = CH, $R^1 = (CH_2)_2(CH_3)_2$, $R^2 = OCH_3$, $R^3 = OCH_3$, R^4 = Cl
5j: X = CH, $R^1 = (CH_2)_2(C_2H_5)_2$, $R^2 = OCH_3$, $R^3 = OCH_3$, R^4 = Cl
5k: X = CH, $R^1 = (CH_2)_2(CH_3)_2$, $R^2 = OCH_3$, $R^3 = OCH_3$, $R^4 = OCH_3$
5l: X = CH, $R^1 = (CH_2)_2(C_2H_5)_2$, $R^2 = OCH_3$, $R^3 = OCH_3$, $R^4 = OCH_3$
5m: X = N, $R^1 = (CH_2)_2(CH_3)_2$, R^2 = H, R^3 = H, R^4 = H
5n: X = N, $R^1 = (CH_2)_2(C_2H_5)_2$, R^2 = H, R^3 = H, R^4 = H
5o: X = N, $R^1 = (CH_2)_2(CH_3)_2$, R^2 = H, $R^3 = OCH_3$, R^4 = H
5p: X = N, $R^1 = (CH_2)_2(C_2H_5)_2$, R^2 = H, $R^3 = OCH_3$, R^4 = H
5q: X = N, $R^1 = (CH_2)_2(CH_3)_2$, R^2 = H, R^3 = Cl, R^4 = H
5r: X = N, $R^1 = (CH_2)_2(C_2H_5)_2$, R^2 = H, R^3 = Cl, R^4 = H
5s: X = N, $R^1 = (CH_2)_2(CH_3)_2$, $R^2 = OCH_3$, $R^3 = OCH_3$, R^4 = H
5t: X = N, $R^1 = (CH_2)_2(C_2H_5)_2$, $R^2 = OCH_3$, $R^3 = OCH_3$, R^4 = H

Reagents and conditions: (**i**) HCl 18%/$NaNO_2$/H_2O/0 °C; (**ii**) AcONa, MeOH; (**iii**) EtOH HCl, ∆; (**iv**) $ClCH_2CH_2N(R)_2$ HCl, NaH, DMF, ∆.

2.2 Antiproliferative activity

The antiproliferative activity of the newly synthesized derivatives was evaluated *in vitro* on three human tumor cell lines: HeLa (cervix adenocarcinoma), A-431 (squamous carcinoma), and MSTO-211H (biphasic mesothelioma) cells. The results, expressed as GI_{50} values, i.e. the concentration (μM) of compound able to produce 50% cell death with respect to the control culture, are reported in Table 1. The potent antitumor agent ellipticine was used as a reference compound, in view of its structural similarity to the newly synthesized derivatives **5a-t** [30].

All the tested compounds exert a significant antiproliferative activity on the considered cell lines, showing GI_{50} values ranging from 0.31 to 6.93 μM, which are in some cases comparable to those obtained for ellipticine. In general, HeLa cells seem to be less sensitive than A431 and MSTO-211H cell lines, which actually display the lower GI_{50} values. Moreover, in most cases, the antiproliferative effect exerted by the compounds featuring a dimethylaminoethyl side chain at R^1 appears higher with respect to that exerted by the corresponding analogues characterized by the diethylaminoethyl group. In details, the most active benzothiopyranoindoles are **5g** and **5k**, while, within the pyridothiopyranoindole subseries, the most cytotoxic derivatives are **5m** and **5s**. Interestingly, from a structural point of view, all compounds are characterized by a dimethylaminoethyl side chain, and three out of four (**5g**, **5k**, **5s**) bear methoxy groups at R^2 and R^3 positions.

Considering the benzothiopyranoindole derivatives (compounds **5a-l**) an important role seems to be played by the group at the R^2-position. Indeed, the substitution of the hydrogen with a methoxy group at this position induces a significant increase in cytotoxicity, as demonstrated by comparing the antiproliferative activity of **5a** and **5b** with that exerted by **5g** and **5h**, respectively. Interestingly, for compound **5g** an increase in cytotoxicity of about 7-fold with respect to the congener **5a** was observed in all three human tumor cell lines taken into consideration. The addition of a further methoxy substituent at R^4 does not influence appreciably the antiproliferative profile of both **5g** and **5h**, as their analogues **5k** and **5l** show comparable GI_{50} values.

Table 1. Antiproliferative activity of the new compounds **5a-t** and ellipticine taken as reference.

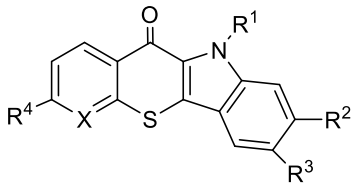

n	X	R^1	R^2	R^3	R^4	GI_{50} (μM)		
						HeLa	A-431	MSTO-211H
5a	CH	$CH_2CH_2N(CH_3)_2$	H	OCH_3	H	5.81± 0.59	2.24± 1.68	2.37± 0.30
5b	CH	$CH_2CH_2N(CH_2CH_3)_2$	H	OCH_3	H	2.79 ± 0.71	2.08 ± 0.09	1.61 ± 0.28
5c	CH	$CH_2CH_2N(CH_3)_2$	H	OCH_3	Cl	2.79 ± 0.95	2.67 ± 0.46	2.96 ± 0.05
5d	CH	$CH_2CH_2N(CH_2CH_3)_2$	H	OCH_3	Cl	3.21 ± 0.26	5.44 ± 0.48	4.19 ± 0.14
5e	CH	$CH_2CH_2N(CH_3)_2$	H	Cl	Cl	2.66 ± 0.74	1.76 ± 0.68	1.64 ± 0.55
5f	CH	$CH_2CH_2N(CH_2CH_3)_2$	H	Cl	Cl	4.31 ± 1.15	3.29 ± 1.71	2.99 ± 0.11
5g	CH	$CH_2CH_2N(CH_3)_2$	OCH_3	OCH_3	H	0.82 ± 0.04	0.33 ± 0.06	0.31 ± 0.03
5h	CH	$CH_2CH_2N(CH_2CH_3)_2$	OCH_3	OCH_3	H	1.77 ± 0.32	1.11 ± 0.38	0.70 ± 0.05
5i	CH	$CH_2CH_2N(CH_3)_2$	OCH_3	OCH_3	Cl	3.54 ± 0.41	3.19 ± 0.56	1.82 ± 0.61
5j	CH	$CH_2CH_2N(CH_2CH_3)_2$	OCH_3	OCH_3	Cl	4.55 ± 0.39	2.22 ± 0.80	2.37 ± 0.48
5k	CH	$CH_2CH_2N(CH_3)_2$	OCH_3	OCH_3	OCH_3	0.74 ± 0.13	0.48 ± 0.10	0.44 ± 0.15
5l	CH	$CH_2CH_2N(CH_2CH_3)_2$	OCH_3	OCH_3	OCH_3	1.75 ± 0.45	0.67 ± 0.14	0.36 ± 0.05
5m	N	$CH_2CH_2N(CH_3)_2$	H	H	H	1.55 ± 0.05	0.54 ± 0.04	1.08 ± 0.07
5n	N	$CH_2CH_2N(CH_2CH_3)_2$	H	H	H	2.57 ± 0.21	0.47 ± 0.02	1.33 ± 0.06
5o	N	$CH_2CH_2N(CH_3)_2$	H	OCH_3	H	2.71 ± 0.53	1.42 ± 0.26	0.75 ± 0.27
5p	N	$CH_2CH_2N(CH_2CH_3)_2$	H	OCH_3	H	2.61± 1.04	1.90 ± 0.21	0.70 ± 0.06
5q	N	$CH_2CH_2N(CH_3)_2$	H	Cl	H	3.02 ± 0.82	2.00 ± 0.35	2.36 ± 0.46
5r	N	$CH_2CH_2N(CH_2CH_3)_2$	H	Cl	H	4.20 ± 0.36	1.79 ± 0.05	1.42 ± 0.09
5s	N	$CH_2CH_2N(CH_3)_2$	OCH_3	OCH_3	H	1.70 ± 0.01	0.71 ± 0.28	0.35 ± 0.03
5t	N	$CH_2CH_2N(CH_2CH_3)_2$	OCH_3	OCH_3	H	6.93 ± 1.14	2.67 ± 1.66	0.62 ± 0.01
Ellipticine						0.47 ± 0.12	0.65 ± 0.15	0.77 ± 0.14

Nevertheless, the R^2 position lacks to be determinant for cytotoxicity if a chlorine is present at R^4. Indeed, the insertion of a methoxy group at R^2 in **5c** and **5d** to obtain **5i** and **5j**, does not induce any appreciable change in the GI_{50} values. It could be speculated that the presence of the chlorine at R^4 provokes a detrimental effect, which prevails on the advantageous influence mediated by the methoxy substituent at R^2.

The comparison between the effect exerted by **5c** and **5d** with that of **5e** and **5f**, respectively, highlighted no significant differences in cytotoxicity, suggesting for the R^3 position a less relevant role.

As regards the pyridothiopyranoindole derivatives **5m-t**, the lower GI_{50} values are showed by the unsubstituted **5m** and by derivative **5s**, characterized by the presence of two methoxy groups at R^2 and R^3 and by the dimethylaminoethyl side chain at R^1. In particular, antiproliferative activity induced by **5m**, that is slightly decreased by the insertion of a methoxy group at R^3 in compound **5o**, is recovered when a further methoxy is present at R^2-position, as in **5s**. The detrimental effect of the insertion of a chlorine inserted at position R^3 appears confirmed also for pyridothiopyranoindole subseries: in all three tested cell lines, the cytotoxic effect of **5q** and **5r** is lower with respect to that obtained for **5m** and **5n**.

Finally, preliminary viability experiments performed on the non-tumorigenic mesothelial cells Met5-A for some representative compounds, i.e. **5a**, **5g**, **5o** and **5s**, as expected, did not permit to demonstrate any significant selectivity against tumor cells over the nonmalignant ones (data not shown). These results are not surprising, as Topoisomerase poisons are all known to suffer from limited tumor selectivity [23]. However, nowadays, a number of tumor delivering nanotechnologies have been implemented and allow for a preferential tumor distribution (Trojan horse approach) [23].

2.3 Evaluation of Cell Death

To investigate the cell death pathway, cytofluorimetric evaluations on HeLa cells labeled with Annexin V and propidium iodide, and treated for 18 h with the most cytotoxic benzothiopyranoindole **5g** were performed. The results are shown as dot plots in Figure 1. The incubation in the presence of **5g** causes a dose-dependent decrease in viability and a concurrent increase in apoptotic cells. In detail, the percentage of viable cells diminishes from 91.6% (control) to less than 50% at 80 μM concentration. Accordingly, the percentage of apoptotic cells, both early and late apoptosis, increases from 7.8% to about 48% in the same experimental conditions.

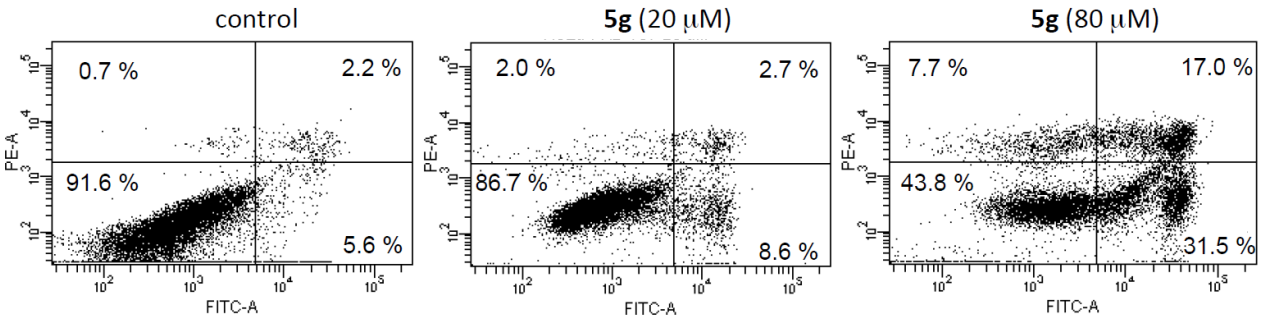

Figure 1. Dual parameter cytogram of FITC-annexin V vs propidium iodide staining. HeLa cells were incubated for 18 h in the absence (control) and in the presence of **5g** at 20 and 80 μM concentration as indicated.

2.4 Interaction with DNA

To investigate the mechanism of action responsible for the cytotoxic activity of the new benzothiopyranoindole and pyridothiopyranoindole derivatives **5a-t**, linear flow dichroism (LD) experiments were performed. As an example, the LD spectra of an aqueous solution of salmon testes DNA alone and in the presence of **5g** and **5s** at different [drug]/[DNA] ratios are shown in Figure 2A and 2B, respectively. Compounds **5g** and **5s** were selected as representatives of the benzothiopyranoindole and pyridothiopyranoindole subseries, respectively, in virtue of their high antiproliferative activity (Table 1). The LD spectra of DNA in the presence of ellipticine were reported as reference (Figure 2C).

The DNA LD spectrum shows the typical negative dichroic signal at 260 nm (lines a). In the presence of test compounds at 0.02 and 0.04 [drug]/[DNA] ratios (lines b and c, respectively), the occurrence of a negative dichroic signal at wavelengths higher (330-450 nm) than that due to DNA bases indicates the ability of both the benzothiopyranoindole and pyridothiopyranoindole chromophores to form a molecular complex with DNA. Moreover, the negative sign of this LD induced signal suggests an orientation of the planar chromophore parallel to the plane of DNA bases, i.e. an intercalative mode of binding, in agreement with the spectra of DNA in the presence of ellipticine, a well-known

intercalative compound (Figure 2C). Similar behaviours have been observed for all the new derivatives (Figures S2-S5, Supporting Information, SI).

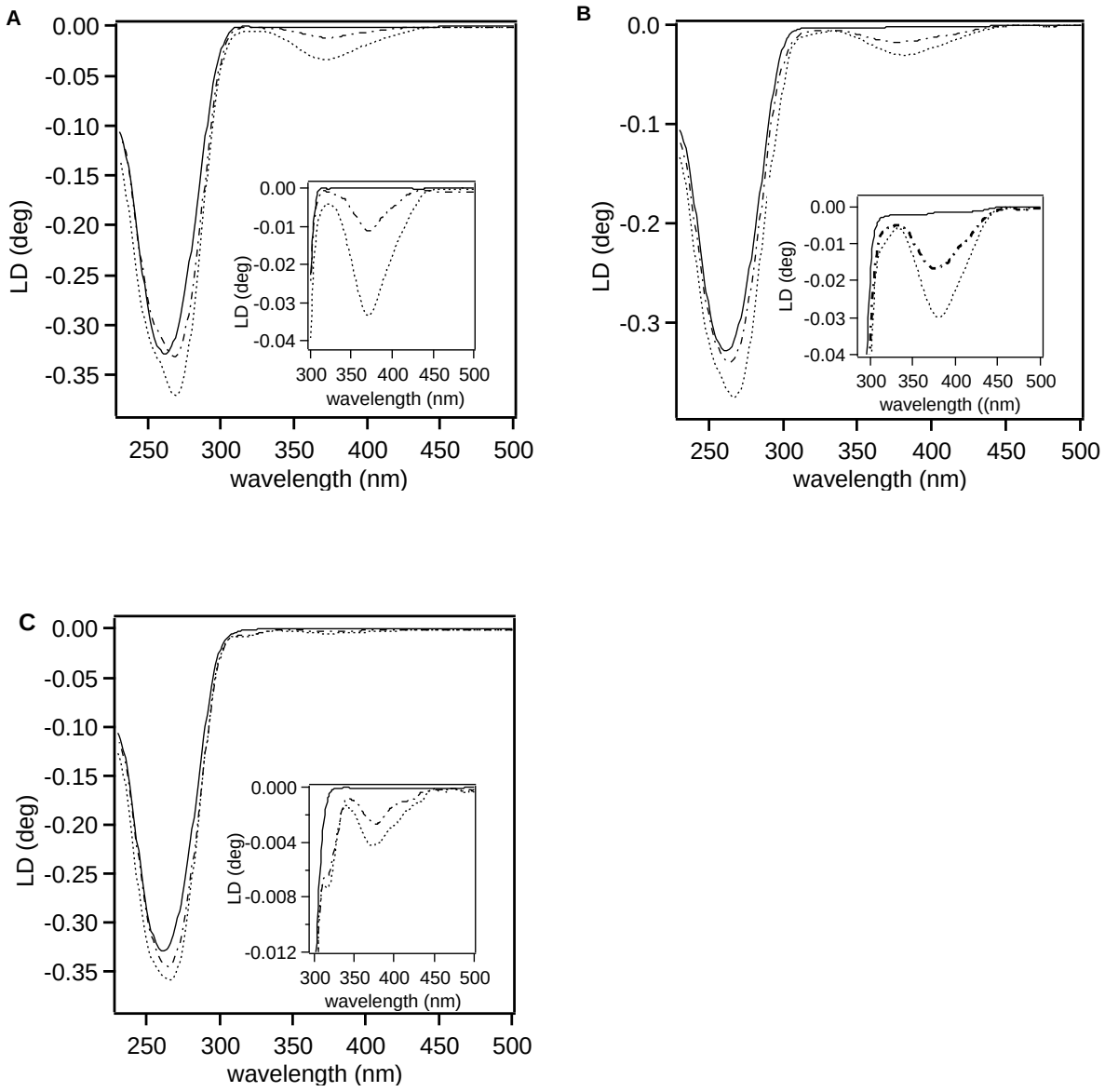

Figure 2. Linear flow dichroism (LD) spectra for compound **5g** (A), **5s** (B) and ellipticine (C) at [drug]/[DNA] ratios = 0.00 (a), 0.02 (b) and 0.04 (c). [DNA]=1.9 x10^{-3}M in ETN buffer.

2.5 Effect on Topoisomerase Activity

Considering that DNA Topoisomerases constitute the molecular intracellular target of many anticancer drugs, including known DNA intercalators, such as adriamycin, *m*-amsacrine (*m*-AMSA) and mitoxantrone [5,18], the effect of the new derivatives on the relaxation of supercoiled plasmid pBR322 DNA mediated by both Topo II and Topo I was also investigated.

In particular, Figure 3A and 3B report the effect of **5g** and **5s** on the relaxation of pBR322 supercoiled DNA catalyzed by Topo II, respectively. Both derivatives are able to inhibit the formation of topoisomers catalyzed by the enzyme from supercoiled DNA (DNA). This effect is concentration-dependent and both derivatives are able to induce a practically complete inhibitory effect at 50 μM concentration.

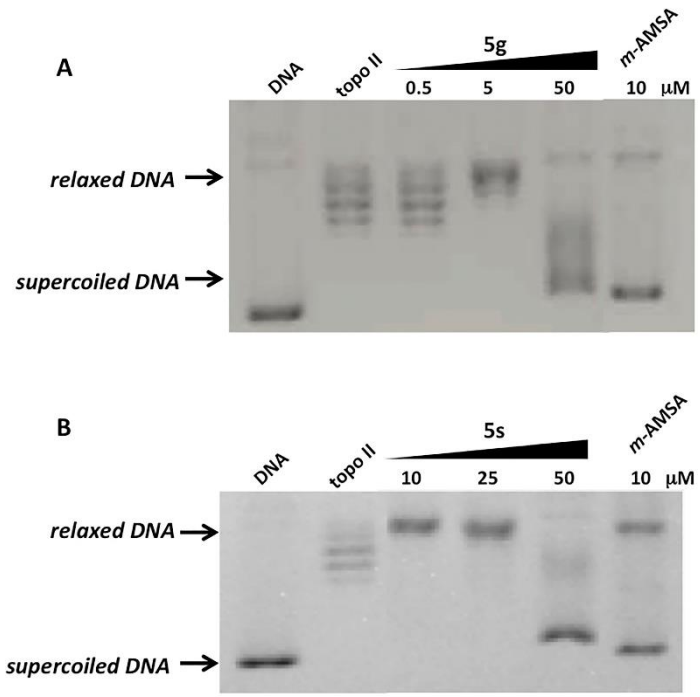

Figure 3**.** Effect on relaxation of supercoiled pBR322 DNA mediated by Topo II. Supercoiled DNA (DNA) was incubated with Topo II in the absence (topo II) and presence of **5g** (A) or **5s** (B) at indicated concentrations (μM); 10 μM *m*-AMSA was used as reference.

A similar behavior was also observed by incubating Topo I with the same derivatives **5g** and **5s** (Figure 4A and 4B, respectively). In particular, by increasing the concentration of the compounds, a dose-dependent decrease in the number of topoisomers appears.

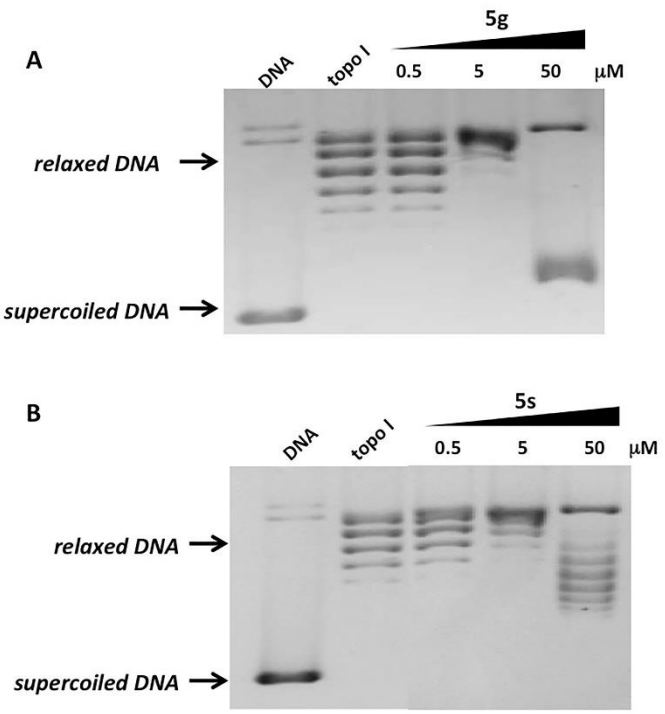

Figure 4. Effect on relaxation of supercoiled pBR322 DNA by human recombinant Topo I. Supercoiled DNA (DNA) was incubated with Topo I in the absence (topo I) and presence of **5g** (A) and **5s** (B) at indicated concentrations (μM).

It is to underline that all the new derivatives, both benzothiopyranoindoles (**5a-l**) and pyridothiopyranoindoles (**5m-t**) showed a concentration-dependent ability to inhibit the relaxation activity of both Topo II and Topo I (data not shown), suggesting a possible relationship with the shared intercalative capacity. Thus, it seems reasonable to assume that the intercalation of the planar tetracyclic chromophore inside base pairs could interfere with the ability of both enzymes to relax supercoiled DNA.

The most clinically relevant intercalative anticancer drugs are able to affect the catalytic cycle of topoisomerases by stabilizing a covalent intermediate, named cleavable complex, thus converting topoisomerase into a cellular poison. Notably, this ability, also referred as poisoning effect, is retained of crucial importance for the anticancer properties of both anti-Topo II (e.g. doxorubicin and *m*-AMSA) and anti-Topo I (e.g. **2** and **3**) drugs.

In this connection, further experiments were performed to verify the ability of the new derivatives to promote the formation of the cleavable complex, in the presence of both Topo II and Topo I. From an experimental point of view, the cleavable complex can be evidenced by the enzyme-mediated formation of linear (Topo II) or nicked (Topo I) DNA from supercoiled one in the presence of test compounds.

Figure 5 shows the results of the cleavable assay performed in the presence of Topo II incubated with the benzothiopyranoindole **5g** and the pyridothiopyranoindole **5s**. The well-known Topo II poison *m*-AMSA was used as reference compound. Both compounds are unable to induce any poison effect up to 50 μM concentration, as demonstrated by the absence of linear DNA, which is otherwise detectable in the presence of the reference drug already at 10 μM. Similar results were obtained also for the other benzothiopyranoindole and pyridothiopyranoindole derivatives (data not shown).

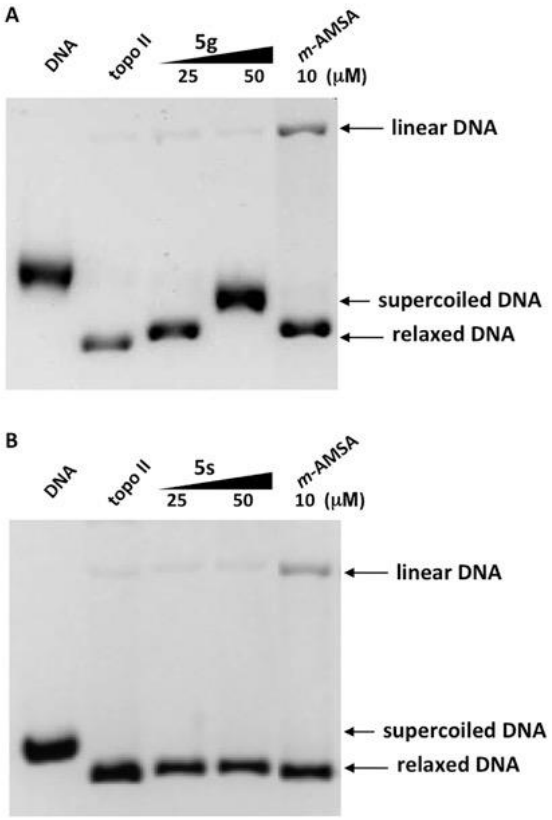

Figure 5. Effect on the stabilization of covalent DNA-Topo II complex. Supercoiled pBR322 DNA (DNA) was incubated with Topo II in the absence (topo II) and presence of **5g** (A) or **5s** (B) at indicated concentration (μM); 10 μM *m*-AMSA was used as reference drug.

Figure 6 reports the results from the cleavable assay performed with Topo I in the presence of **5g** (A) and **5s** (B), and the structurally related analogues **5h** (A) and **5t** (B), respectively. Compound **1** (CPT) was used as reference. The cleavable complex can be evidenced by the enzyme-mediated formation of nicked DNA from supercoiled one in the presence of test compounds. As expected, **1** induces the formation of a significant amount of nicked DNA, i.e. stabilizes the cleavable complex.

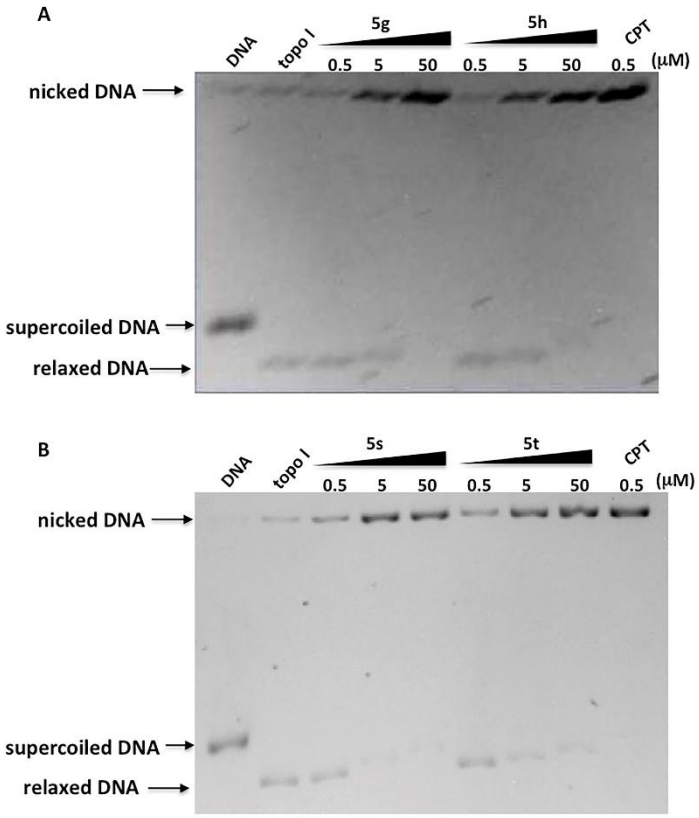

Figure 6. Effect on the stabilization of covalent DNA-Topo I complex. Supercoiled pBR322 DNA (DNA) was incubated with Topo I in the absence (topo I) and presence of **5g** and **5h** (A), **5s** and **5t** (B) at indicated concentration (μM). 0.5 μM **1** (CPT) was used as reference.

Notably, also in the presence of **5g** and **5s** a dose-dependent poisoning effect is observed, as demonstrated by the occurrence of nicked DNA. Interestingly, the evaluation of the effect on the stabilization of cleavable complex performed with all the new derivatives highlighted this ability also for the corresponding analogues **5h** and **5t**, carrying the same methoxy substituents at R^2 and R^3, but the diethylaminoethyl side chain at R^1 (Figure 6A and 6B, respectively). It is noteworthy that all the

other benzothiopyranoindole and pyridothiopyranoindole derivatives appear unable to exert any poisoning effect on Topo I (results not shown).

2.6 Molecular Modeling Studies

The analysis of human Topo I covalently bound to duplex DNA and in complex with **2** (PDB code: 1K4T) [33] or other inhibitors (SA315F, MJ238, AI-III-52, PDB codes: 1SEU, 1SC7, 1TL8), revealed that there are certain strictly conserved contacts between the known ligands and the protein, that can be either direct- or water-mediated- interactions. For this reason, we decided to run docking calculations explicitly considering the water molecules, using the Autodock4.2 software (AD4) [34]. In this regard, AD4 has been implemented with a new force field and with a hydration docking method able to predict waters mediating ligand binding [35]. Such a protocol has been already used by us to successfully reproduce the experimental binding conformation of **2** and to rationalize the Topo I inhibitory activity of pyrazoloquinazoline derivatives [29]. The poisons **5g**, **5h**, **5s** and **5t** were docked in the high resolution (2.10 Å) crystal structure of the human Topo I in complex with duplex DNA/**2** (PDB code: 1K4T, see Experimental Section for the selection criteria) [33] after removal of the poison. Analyzing, for each docked molecule, the lowest energy binding pose in the most populated family, it emerges that **5g**, **5h**, **5s** and **5t** docks similarly. All the obtained complexes were energy minimized as to allow the water molecules to adjust and the ligand to optimize its geometries of interactions, and the protein to remove its internal bad contacts. Particularly, **5g** (likewise **5h**, **5s** and **5t**) docks at the DNA cleavage site (Figure 7), where its benzothiopyrano fragment stacks with the non-cleaved strand bases (+1C and -1A) and the indole ring stacks with the scissile strand site of the duplex DNA (+1G and -1T bases) similarly to other CPT-like Topo I poisons. Noteworthy, a water bridge is found between the R^3-methoxy oxygen and the K751 side chain and two H-bonds are detected: one between the **5g** carbonyl oxygen and the Topo I R364 side chain, and another between the **5g** R^2-methoxy oxygen and the amide of the N722 side chain. These two H-bonds are strictly conserved among the CPTs, indolocarbazoles, and indenoisoquinolines poisons and, together with

the extensive stacking interactions, are crucial for an efficient bonding to the DNA-Topo I cleavage complex. In fact, mutations of the above mentioned residues are known to confer resistance to CPT-like [36] and non-CPT-like poisons [37-39]. The importance of these H-bonds would be in line with the inability to exert a poisoning effect of our analogues **5a**-**5f** and **5m**-**5r**, which, lacking of a H-bond acceptor at the R^2 position, are not able to establish a contact with the N722 side chain. Furthermore, in the docking pose predicted for **5g** (and **5s**), the R^1-dimethylaminoethyl branch is found in a small and rather shallow protein pocket in proximity of the catalytic phosphotyrosine (pY) and the DNA phosphodiester backbone, where the **5g** protonated amino group is able to establish a water-mediated contact with the D533 side chain (**2** establishes a direct interaction). The size of the pocket is sufficient to fit the R^1-diethylaminoethyl moiety of the **5h** and **5t** derivatives, which are still able to establish the same water-mediated interaction. However, given the lower cytotoxicity exerted by these two analogues on the three tumor cell lines used in our assays, it seems that the larger diethylamino group (**5h** and **5t**) would be less tolerated with respect to the dimethylamino one, although other in-cell effects could also explain the observed results.

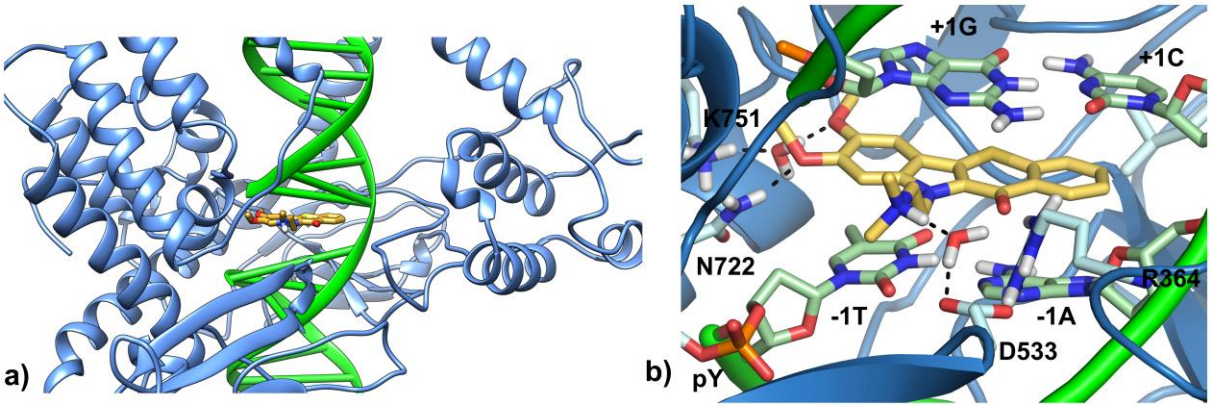

Figure 7. A zoomed-out (a) and zoomed-in (b) view of the minimized putative binding mode of **5g** (golden sticks) into the DNA (green ribbon) cleavage site of Topo I (blue ribbon). The protein interacting residues and the DNA bases are depicted as light-blue and light-green sticks, respectively. H-bonds are depicted as dashed black lines.

The results presented herein can also explain the catalytic inactivity of compounds **5i**-**5l**. In fact, according to the described binding pose, the R^4 substituent of these derivatives is oriented toward the non-scissile DNA strand, where several evidences indicate that a steric hindrance in the ligand is extremely poorly tolerated (see also Figure S1, Supporting Information) [40]. Molecular docking of a R^4-substituted-compound, like **5k**, confirmed in fact, that the ligand is not able to accommodate into the binding pocket anymore and none of the aforementioned conserved H-bonds can be established.

In conclusion, the theoretical model provided by hydrated docking calculations well clarified the molecular determinants that translate DNA intercalation into Topo I poison activity. Importantly, it has been revealed that only compounds possessing a H-bond acceptor at the R^2-position can effectively interact with the complex and that bulky substituents at the R^4-position do not allow a proper accommodation. The identification of these structural requirements can be useful for the future development of novel series of antiproliferative agents acting as Topo I poisons.

3. Conclusions

As a continuation of our studies aimed to identify new antiproliferative agents, novel benzothiopyranoindole (**5a-l**) and pyridothiopyranoindole (**5m-t**) derivatives featuring different substitution patterns at R^2-R^4 positions and protonatable dialkylaminoalkyl chains at R^1-position, were synthesized and biologically evaluated on a panel of three human tumor cell lines, showing evident cytotoxic (GI_{50} values in the low micromolar/submicromolar range) and pro-apoptotic effects. Further investigations revealed that the tetracyclic chromophores allow a complexation with DNA through an intercalative mode of binding and this ability could be considered responsible for the capacity of all derivatives to inhibit the DNA relaxation activity mediated by both Topo II and Topo I. More interestingly, the presence of a methoxy group at R^2-position of both chromophores seems to play a crucial role in the ability to stabilize the cleavable complex formed by the catalytic activity of Topo I, conferring Topo I poison properties. A theoretical model provided by hydrated docking

calculations clarified the molecular determinants responsible for the Topo I poison activity, rationalizing that only compounds possessing a H-bond acceptor at the R^2-position can effectively interact with the complex and that bulky substituents at the R^4-position do not allow a proper accommodation.

The results obtained so far highlight the benzothiopyranoindole and the isoster pyridothiopyranoindole systems as excellent scaffolds for the development of antiproliferative agents, and furnish crucial indications about the structural requirements suitable for the future design of novel efficacious Topo I poisons.

4. Experimental protocols

4.1. Chemistry

The uncorrected melting points were determined using a Reichert Köfler hot-stage apparatus. ^{1}H NMR and ^{13}C NMR spectra were recorded on a Varian Gemini 200 spectrometer (^{1}H, 200 MHz) in dimethyl-d_6 sulfoxide or on a Bruker AVANCE 400 (^{1}H, 400 MHz; ^{13}C, 100 MHz) in $CDCl_3$. The coupling constants (*J*) are given in Hertz. Accurate molecular weights of compounds were confirmed by ESI mass spectrometry using a ThermoFisher Scientific Orbitrap XL mass spectrometer in electrospray positive ionization modes (ESI-MS). Magnesium sulphate was used as the drying agent. Evaporations were made in vacuo (rotating evaporator). Analytical TLC have been carried out on Merck 0.2 mm precoated silica gel aluminium sheets (60 F-254). Silica gel 60 (230-400mesh) was used for column chromatography. Purity of the target inhibitors was determined, using a Shimadzu LC-20AD SP liquid chromatograph equipped with a DDA Detector at 288 nm and 340 nm (column C18 (250 mm-4.6 mm, 5 μm, Shim-pack)). The mobile phase, delivered at isocratic flow, consisted of acetonitrile (70–90%) and water (30–10%) and a flow rate of 1.0 mL/min. All the compounds showed percent purity values of ≥ 95%. Reagents, starting materials, and solvents were purchased from commercial suppliers and used as received. The following compounds were obtained according to methods previously described: 3-(hydroxymethylene)-2*H*-thiopyran-4(3*H*)-one **6a** [31], 3-

(hydroxymethylene)-7-methoxy-2*H*-thiopyran-4(3*H*)-one **6b**, and 3-(hydroxymethylene)-7-chloro-2*H*-thiopyran-4(3*H*)-one **6c** [30], 2,3-dihydro-3-(hydroxymethylene)-thiopyrano[2,3-*b*]pyridin-4(4*H*)-one, **6d**, 3–(2-phenylhydrazono)-2*H*-thiopyrano[2,3-*b*]pyridin-4(3*H*)-one **8g**, 3–[2-(4-methoxyphenyl)hydrazono]-2*H*-thiopyrano[2,3-*b*]pyridin-4(3*H*)-one **8h**, 3–[2-(4-chlorophenyl)hydrazono]-2*H*-thiopyrano[2,3-*b*]pyridin-4(3*H*)-one **8i,** pyrido[3',2':5,6]thiopyrano[3,2-*b*]indol-5(6*H*)-one **9g**, 9-methoxy-pyrido[3',2':5,6]thiopyrano[3,2-*b*]indol-5(6*H*)-one, **9h** and 9-chloro-pyrido[3',2':5,6]thiopyrano[3,2-*b*]indol-5(6*H*)-one, **9i** [27].

*4.1.1. General synthetic procedure for 7-substituted-3-(2-phenylhydrazono)-2H-benzothiopyran-4(3H)-ones **8a-f** and 3–[2-(3,4-dimethoxyphenyl)hydrazono]thiopyrano[2,3-b]pyridin-4(3H)-one **8j**.*

To a solution of 4.5 mmol of the appropriate compound **6a-d** in 30 mL of methanol was added an aqueous saturated solution of 14.0 mmol of sodium acetate. After cooling at 0 °C, a solution of the suitable diazonium salt, obtained from the appropriately substituted aniline **7a-d** in 18% hydrochloridric acid and sodium nitrite, was added dropwise in slight excess (6.0 mmol). An orange precipitate was immediately formed, and the mixture was stirred for 30 min at room temperature. The solid was collected and washed with water to give compounds **8a-f** and **8j**.

*4.1.1.1. 3-[2-(4-Methoxyphenyl)hydrazono]-2H-benzothiopyrano-4(3H)-one (**8a**).*Yield, 75 %; m. p. 123-125 °C; ^{1}H-NMR (200 MHz, DMSO-d_6): δ 3.77 (s, 3H), 4.09 (s, 2H), 6.76-6.83 (m, 3H), 6.87-6.91 (m, 3H), 7.01 (d, *J* = 8.4 Hz, 2H), 13.81 (s, 1H, NH exch.) ppm.

*4.1.1.2. 7-Chloro-3-[2-(4-methoxyphenyl)hydrazono]-2H-benzothiopyrano-4(3H)-one (**8b**).* Yield, 70 %; m. p. 136-138 °C; ^{1}H-NMR (200 MHz, DMSO-d_6): δ 3.74 (s, 3H), 4.14 (s, 2H), 6.93-6.97 (m, 2H), 7.29-7.43 (m, 3H), 7.61 (d, *J* = 2.4 Hz, 1H), 7.97 (d, *J* = 8.4 Hz, 1H), 13.82 (s, 1H, NH *exch*.) ppm.

*4.1.1.3. 7-Chloro-3-[2-(4-chlorophenyl)hydrazono]-2H-benzothiopyrano-4(3H)-one (**8c**).* Yield, 80 %; m. p. 168-170 °C; ^{1}H-NMR (200 MHz, DMSO-d_6): δ 4.11 (s, 2H), 6.91-6.99 (m, 2H), 7.33-7.36 (m, 3H), 7.53 (d, *J* = 2.2 Hz, 1H), 7.97 (d, *J* = 8.4 Hz, 1H), 13.45 (s, 1H, NH exch.) ppm.

*4.1.1.4. 3-[2-(3,4-Dimethoxyphenyl)hydrazono]-2H-benzothiopyrano-4(3H)-one (**8d**).* Yield, 80%; m. p. 129-131 °C; ^{1}H-NMR (200 MHz, DMSO-d_6): δ 3.78 (s, 3H), 3.84 (s, 3H), 4.10 (s, 2H), 6.76-6.83 (m, 3H), 6.87-6.91 (m, 3H), 7.18 (s, 1H), 13.84 (s, 1H, NH exch.) ppm.

*4.1.1.5. 7-Chloro-3-[2-(3,4-dimethoxyphenyl)hydrazono]-2H-benzothiopyrano-4(3H)-one (**8e**).* Yield, 65 %; m. p. 142-144 °C; ^{1}H-NMR (200 MHz, DMSO-d_6): δ 3.75 (s, 3H), 3.80 (s, 3H), 4.16 (s, 2H), 6.93-6.97 (m, 2H), 7.16 (s, 1H), 7.42 (dd, J_{min} = 2.0 Hz, J_{max} = 8.2 Hz, 1H), 7.63 (s, 1H), 7.98 (d, J = 8.6 Hz, 1H), 13.83 (s, 1H, NH exch.) ppm.

*4.1.1.6. 7-Methoxy-3-[2-(3,4-dimethoxyphenyl)hydrazono]-2H-benzothiopyrano-4(3H)-one (**8f**).* Yield, 60 %; m. p. 138-140 °C; ^{1}H-NMR (200 MHz, DMSO-d_6): δ 3.73 (s, 3H), 3.81 (s, 3H), 3.86 (s, 3H), 4.09 (s, 2H), 6.81-6.94 (m, 4H), 7.67 (s, 1H), 7.90 (d, J = 8.4 Hz, 1H), 11.52 (s, 1H, NH exch.) ppm.

*4.1.1.7. 3–[2-(3,4-Dimethoxyphenyl)hydrazono]-2H-thiopyrano[2,3-b]pyridin-4(3H)-one (**8j**).* Yield, 60 %; m.p. 174-176 °C; ^{1}H-NMR (200 MHz, DMSO-d_6): δ 3.73 (s, 3H), 3.79 (s, 3H), 4.22 (s, 2H), 6.95-7.00 (m, 2H), 7.16 (s, 1H), 7.35-7.39 (m, 1H), 8.27 (dd, J_{min} = 1.8 Hz, J_{max} = 7.8 Hz, 1H), 8.57 (dd, J_{min} = 1.6 Hz, J_{max} = 4.6 Hz, 1H), 13.80 (s, 1H, NH exch.) ppm.

*4.1.2. General synthetic procedure for substituted-benzothiopyrano[3,2-b]indol-10(11H)-ones **9a-f** and 8,9-dimethoxypyrido[3',2':5, 6]thiopyrano[3,2-b]indol-5(6H)-one **9j.***

A solution of 4.0 mmol of the suitable substituted phenylhydrazone derivatives **8a-f, 8j** in 20 mL of ethanolic hydrogen chloride solution was refluxed for 20 min. After cooling the yellow/light-brown precipitate was collected and washed with ethanol to give crude indoles **9a-f, 9j**, which were purified by recrystallization from DMF.

*4.1.2.1. 3-Methoxybenzothiopyrano[3,2-b]indol-10(11H)-one (**9a**).* Yield, 70 %; m. p. > 300 °C; ^{1}H-NMR (200 MHz, DMSO-d_6): δ 3.84 (s, 3H), 7.16 (d, J = 9.0 Hz, 1H), 7.33 (s, 1H); 7.52 (d, J = 9.0 Hz, 1H), 7.62-7.76 (m, 2H), 8.01 (d, J = 8.4 Hz, 1H), 8.59 (d, J = 8.4 Hz, 1H), 12.39 (s, 1H, NH exch.) ppm.

*4.1.2.2. 7-Chloro-3-methoxybenzothiopyrano[3,2-b]indol-10(11H)-one (**9b**).* Yield, 65 %. m. p. > 300 °C; ^{1}H-NMR (200 MHz, DMSO-d_6): δ 3.86 (s, 3H), 7.17 (dd, J_{min} = 2.2 Hz, J_{max} = 9.0 Hz, 1H), 7.33 (d, J = 2.0 Hz, 1H), 7.53 (d, J = 9.0 Hz, 1H), 7.67 (dd, J_{min} = 2.2 Hz, J_{max} = 8.8 Hz, 1H), 8.25 (d, J = 1.8 Hz, 1H), 8.57 (d, J = 8.8 Hz, 1H), 12.47 (s, 1H, NH exch.) ppm.

*4.1.2.3. 3,7-Dichlorobenzothiopyrano[3,2-b]indol-10(11H)-one (**9c**).* Yield, 40 %; m. p. > 300 °C. ^{1}H-NMR (200 MHz, DMSO-d_6): δ 7.51-7.71 (m, 3H), 8.09 (s, 1H), 8.30 (d, J = 1.8 Hz, 1H), 8.57 (d, J = 8.4 Hz, 1H), 12.79 (s, 1H, NH exch.) ppm.

*4.1.2.4. 2,3-Dimethoxybenzothiopyrano[3,2-b]indol-10(11H)-one (**9d**).* Yield, 75 %; m. p. > 300 °C; ^{1}H-NMR (200 MHz, DMSO-d_6): δ 3.87 (s 6H), 7.02 (s, 1H), 7.32 (s, 1H), 7.58-7.66 (m, 1H), 7.70-7.78 (m, 1H), 7.99 (d, J = 7.2 Hz, 1H), 8.59 (dd, J_{min} = 1.2 Hz. J_{max} = 7.8 Hz, 1H), 12,32 (s, 1H, NH exch.) ppm.

*4.1.2.5. 7-Chloro-2,3-dimethoxybenzothiopyrano[3,2-b]indol-10(11H)-one (**9e**).* Yield, 60 %.; m. p. > 300 °C; ^{1}H-NMR (200 MHz, DMSO-d_6): δ 3.89 (s, 6H), 7.03 (s, 1H), 7.33 (s, 1H), 7.67 (dd, J_{min} = 2.0 Hz, J_{max} = 8.8 Hz, 1H), 8.25 (d, J = 8.8 Hz, 1H), 8.57 (d, J = 9.0 Hz, 1H), 12.39 (s, 1H, NH exch.) ppm.

*4.1.2.6. 2,3,7-Trimethoxybenzothiopyrano[3,2-b]indol-10(11H)-one (**9f**).* Yield, 80 %; m. p. > 300 °C; ^{1}H-NMR (200 MHz, DMSO-d_6): δ 3.87(s, 6H), 3.94 (s, 3H), 7.02 (s, 1H), 7.23 (dd, J_{min} = 2.4 Hz, J_{max} = 8.8 Hz, 1H), 7.26 (s, 1H), 7.48 (d, J = 2.4 Hz, 1H), 8.50 (d, J = 8.8 Hz, 1H), 12.20 (s, 1H, NH exch.) ppm.

*4.1.2.7. 8,9-Dimethoxypyrido[3',2':5,6]thiopyrano[3,2-b]indol-5(6H)-one (**9j**).* Yield, 55 %; m. p. > 300 °C. ^{1}H-NMR (200 MHz, DMSO-d_6): δ 3.88 (s 6H), 7.03 (s, 1H), 7.38 (s, 1H), 7.68 (dd, J_{min} = 4.8 Hz, J_{max} = 7.8 Hz, 1H), 8.86-8.90 (m, 2H), 12.42 (s, 1H, NH exch.) ppm.

*4.1.3. General synthetic procedure for substituted-11-dialkylaminoalkyl-benzothiopyrano[3,2-b]indol-10(11H)-ones **5a-l** and substituted 6-dialkylaminoalkyl-pyrido[3',2':5,6]thiopyrano[3,2-b]indol-5(6H)-ones **5m-t.***

The appropriate compound **9a-j** (0.70 mmol) was added in small portions to a stirred suspension of sodium hydride (60% dispersion in mineral oil, 0.104 g, 2.60 mmol) in 10 mL of anhydrous DMF, under nitrogen atmosphere. The reaction mixture was stirred at room temperature for 2 h and then was supplemented with 1.03 mmol of the appropriate dialkylaminoalkyl chloride hydrochloride and heated at 100 °C for 12-24 h (TLC analysis). After cooling, the obtained suspension was added with water and left to stand at room temperature overnight. The crude products precipitated were collected and purified by recrystallization from DMF.

*4.1.3.1. 11-[2-(Dimethylamino)ethyl]-3-methoxybenzothiopyrano[3,2-b]indol-10(11H)-one (**5a**).* Yield, 30 %; m. p. 107-109 °C; ^{1}H NMR (400 MHz, $CDCl_3$): δ 2.17 (s, 6H), 2.53 (t, *J* = 6.6 Hz, 2H), 3.91 (s, 3H), 5.03 (t, *J* = 6.6 Hz, 2H), 7.17 (d, *J* = 2.4 Hz, 1H), 7.24-7.27 (m, 1H), 7.53-7.59 (m, 2H), 7.64 (td, J_{min} = 1.4 Hz, J_{max} = 8.0 Hz, 1H), 7.77 (d, *J* = 8.0 Hz, 1H), 8.67 (dd, J_{min} = 1.6 Hz, J_{max} = 8.0 Hz, 1H) ppm; ^{13}C-NMR (100 MHz, $CDCl_3$): δ 42.86, 43.23 (2C), 55.68, 56.05, 101.04, 112.03, 119.41, 120.50, 123.09, 126.20, 127.02, 127.61, 128.88, 130.98, 132.40, 134.70, 136.05, 155.06, 173.35 ppm; HRMS (ESI) m/z calculated for $C_{20}H_{21}N_2O_2S([M+H]^+)$ 353.1324, found: 353.1307. Anal. $C_{20}H_{20}N_2O_2S$ (C, H, N).

*4.1.3.2. 11-[2-(Diethylamino)ethyl]-3-methoxybenzothiopyrano[3,2-b]indol-10(11H)-one (**5b**).* Yield, 45 %; m. p. 103-105 °C; ^{1}H NMR (400 MHz, $CDCl_3$): δ 1.12 (t, *J* = 7.2 Hz, 6H), 2.75 (q, *J* = 7.2 Hz, 4H), 2.69 (t, *J* = 6.4 Hz, 2H), 3.92 (s, 3H), 5.03 (t, *J* = 6.4 Hz, 2H), 7.15 (d, *J* = 2.0 Hz, 1H), 7.22 (dd, J_{min} = 2.0 Hz, J_{max} = 9.2 Hz, 1H), 7.51-7.61 (m, 3H), 7.74 (dd, J_{min} = 0.8 Hz, J_{max} = 8.0 Hz, 1H), 8.72 (dd, J_{min} = 1.2 Hz, J_{max} = 8.0 Hz, 1H) ppm; ^{13}C-NMR (100 MHz, $CDCl_3$): δ 14.67 (2C), 42.83 (2C), 51.08, 55.61, 56.09, 100.71, 112.50, 119.36, 120.03, 123.02, 126.07, 127.01, 128.16, 129.08, 130.83, 132.65, 135.13, 136.09, 154.82, 173.33 ppm; HRMS (ESI) m/z calculated for $C_{22}H_{25}N_2O_2S([M+H]^+)$ 381.1637, found: 381.1621. Anal. $C_{22}H_{24}N_2O_2S$ (C, H, N).

*4.1.3.3. 11-[2-(Dimethylamino)ethyl]-7-chloro-3-methoxybenzothiopyrano[3,2-b]indol-10(11H)-one (**5c**).* Yield, 30 %; m. p. 99-101 °C; ^{1}H NMR (400 MHz, $CDCl_3$): δ 2.30 (s, 6H), 2.45 (t, *J* = 7.2 Hz, 2H), 3.92 (s, 3H), 4.89 (t, *J* = 7.4 Hz, 2H), 7.11 (d, *J* = 2.4 Hz 1H), 7.20 (dd, J_{min} =

2.4 Hz, J_{max} = 9.2 Hz, 1H), 7.45 (dd, J_{min} = 2.0 Hz, J_{max} = 8.8 Hz 1H), 7.53 (d, J = 9.2 Hz, 1H), 7.71 (d, J = 2Hz, 1H), 8.61 (d, J = 8.8 Hz, 1H) ppm; ^{13}C-NMR (100 MHz, $CDCl_3$): δ 43.73, 45.14 (2C), 56.00, 56.41, 100.40, 112.37, 117.59, 119.42, 120.08, 122.71, 126.00, 126.65, 127.62, 130.58, 131.09, 135.09, 137.32, 154.78, 173.31 ppm; HRMS (ESI) m/z calculated for $C_{20}H_{20}ClN_2O_2S$ ($[M+H]^+$) 387.0934, found: 387.0911. Anal. $C_{20}H_{19}ClN_2O_2S$ (C, H, N).

*4.1.3.4. 11-[2-(Diethylamino)ethyl]-7-chloro-3-methoxybenzothiopyrano[3,2-b]indol-10(11H)-one (**5d**).* Yield, 35 %; m. p. 95-97 °C; ^{1}H NMR (400 MHz, $CDCl_3$): δ 0.78 (t, J = 7.2 Hz, 6H), 3.06-3.09 (q, 4H), 3.10 (t, J = 6.6 Hz, 2H), 3.89 (s, 3H), 5.23 (t, J = 6.6 Hz, 2H); 7.10 (d, J = 2.0 Hz, 2H), 7.47 (dd, J_{min} = 2.0 Hz, J_{max} = 8.8 Hz, 2H), 7.73 (d, J = 1.6 Hz, 1H), 8.60 (d, J = 8.8 Hz, 1H) ppm; ^{13}C-NMR (100 MHz, $CDCl_3$): δ 14.61 (2C), 47.03 (2C), 51.47, 56.00, 56.47, 100.56, 112.71, 117.83, 119.24, 120.15, 122.36, 126.17, 126.86, 127.43, 130.38, 131.01, 134.87, 137.21, 154.63, 173.29 ppm; HRMS (ESI) m/z calculated for $C_{22}H_{24}ClN_2O_2S$ ($[M+H]^+$) 415.1247, found: 415.1234. Anal. $C_{22}H_{23}ClN_2O_2S$ (C, H, N).

*4.1.3.5. 11-[2-(Dimethylamino)ethyl]-3,7-dichlorobenzothiopyrano[3,2-b]indol-10(11H)-one (**5e**).* Yield, 40 %; m. p. 183-185 °C; ^{1}H-NMR (400 MHz, $CDCl_3$): δ 2.99 (s, 6H), 3.51 (t, J = 6.4 Hz, 2H), 5.44 (t, J = 6.6 Hz, 2H), 7.46-7.54 (m, 2H), 7.74-7.83 (m, 2H), 8.13 (d, J = 9.0 Hz, 1H), 8.58 (d, J = 9.0 Hz, 1H) ppm; ^{13}C-NMR (100 MHz, $CDCl_3$): δ 43.64, 45.71 (2C), 57.03, 100.89, 111.94, 117.98, 119.86, 121.02, 123.45, 126.33, 127.59, 128.45, 130.86, 131.15, 134,03, 137.17, 155.04, 172.81 ppm; HRMS (ESI) m/z calculated for $C_{19}H_{17}Cl_2N_2OS$ ($[M+H]^+$) 391.0439, found: 391.0420. Anal. $C_{19}H_{16}Cl_2N_2OS$ (C, H, N).

*4.1.3.6. 11-[2-(Diethylamino)ethyl]-3,7-dichlorobenzothiopyrano[3,2-b]indol-10(11H)-one (**5f**).* Yield, 40 %; m. p. 137-139 °C; ^{1}H NMR (400 MHz, $CDCl_3$): δ 1.53 (t, J = 7.2 Hz, 6H), 3.27 (q, J = 7.2 Hz, 4H), 3.44 (t, J = 6.4 Hz, 2H), 5.46 (t, J = 6.6 Hz, 2H), 7.50-7.520 (m, 2H), 7.60 (d, J = 8.4 Hz, 1H), 7.80 (d, J = 2.0 Hz, 1H), 8.26 (d, J = 8.4 Hz,1H), 8.60 (d, J = 9.0 Hz, 1H) ppm; ^{13}C-NMR (100 MHz, $CDCl_3$): δ 14.63 (2C), 47.70 (2C), 52.02, 57.14, 101.58, 113.70,

117.94, 119.79, 120.06, 123.64, 126.46, 127.40, 128.48, 130.45, 131.09, 134.05, 137.12, 154.83, 172.84 ppm; HRMS (ESI) m/z calculated for $C_{21}H_{21}Cl_2N_2OS$ ($[M+H]^+$) 419.0752, found: 419.0730. Anal. $C_{21}H_{20}Cl_2N_2OS$ (C, H, N).

*4.1.3.7. 11-[2-(Dimethylamino)ethyl]-2,3-dimethoxybenzothiopyrano[3,2-b]indol-10(11H)-one (**5g**).* Yield, 25 %; m. p. 120-122 °C; ^{1}H NMR (400 MHz, $CDCl_3$): δ 2.93 (s, 6H), 2.56 (t, *J* = 6.8 Hz, 2H), 4.01 (s, 3H), 4.19 (s, 3H), 5.42 (t, *J* = 6.8 Hz, 2H), 7.10 (s, 1H), 7.56 (t, *J* = 7.0 Hz, 1H), 7.64 (td, J_{min} = 1.4 Hz, J_{max} = 8.0 Hz, 1H), 7.76-7.79 (m, 2H); 8.66 (dd, J_{min} = 1.2 Hz, J_{max} = 8.0 Hz, 1H) ppm; ^{13}C-NMR (100 MHz, $CDCl_3$): δ 41.30 (2C), 43.83, 56.52, 57.32 57.90, 93.91, 100.25, 115.16, 119.86, 126.34, 126.61, 127.05, 128.54, 130.84, 135,82, 135.81, 135.92, 146.97, 153.01, 172.23 ppm; HRMS (ESI) m/z calculated for $C_{21}H_{23}N_2O_3S$ ($[M+H]^+$) 383.1429, found: 383.1408. Anal. $C_{21}H_{22}N_2O_3S$ (C, H, N).

*4.1.3.8. 11-[2-(Diethylamino)ethyl]-2,3-dimethoxybenzothiopyrano[3,2-b]indol-10(11H)-one (**5h**).* Yield, 40 %; m. p. 105-107 °C; ^{1}H NMR (400 MHz, $CDCl_3$): δ 1.24 (t, *J* = 7.2 Hz, 6H), 2.91 (q, *J* = 7.2 Hz, 4H), 3.12 (t, *J* = 7.2 Hz, 2H), 3.98 (s, 3H), 4.08 (s, 3H), 5.12 (t, *J* = 7.2 Hz, 2H), 7.07 (s, 1H), 7.34 (s, 1H), 7.51 (td, J_{min} = 1.2 Hz, J_{max} = 8.0 Hz, 1H), 7.58 (td, J_{min} = 1.4 Hz, J_{max} = 8.0 Hz, 1H), 7.71 (d, *J* = 7.6 Hz, 1H), 8.68 (dd, J_{min} = 1.4 Hz, J_{max} = 8.2 Hz, 1H) ppm; ^{13}C-NMR (100 MHz, $CDCl_3$): δ 10.75 (2C), 47.40 (2C), 52.74, 56.50, 56.64, 57.26, 93.50, 100.48, 115.42, 119.92, 126.18, 126.56, 127.02, 128.93, 130.70, 132.56, 135.72, 135.86, 146.62, 152.88, 172.29 ppm; HRMS (ESI) m/z calculated for $C_{23}H_{27}N_2O_3S$ ($[M+H]^+$) 411.1742, found: 411.1725. Anal. $C_{23}H_{26}N_2O_3S$ (C, H, N).

*4.1.3.9. 11-[2-(Dimethylamino)ethyl]-7-chloro-2,3-dimethoxybenzothiopyrano[3,2-b]indol-10(11H)-one (**5i**).* Yield, 25 %; m. p. 170-172 °C; ^{1}H NMR (400 MHz, $CDCl_3$): δ 2.43 (s, 6H), 2.80 (t, *J* = 7.4 Hz, 2H), 3.98 (s, 3H), 4.02 (s, 3H), 4.95 (t, *J* = 7.4 Hz, 2H), 6.97 (s, 1H), 7.03 (s, 1H), 7.42 (dd, J_{min} = 2.0 Hz, J_{max} = 8.8 Hz, 1H), 7.65 (d, *J* = 2.0 Hz, 1H), 8.59 (d, *J* = 8.8 Hz, 1H) ppm; ^{13}C-NMR (100 MHz, $CDCl_3$): δ 43.90, 45.77 (2C), 56.48, 56.55, 59.28, 92.58,

100.33, 115.29, 118.62, 125.85, 126.33, 126.55, 130.39, 130.96, 135.41, 136.91, 136.97, 146.43, 152.52, 171.29 ppm; HRMS (ESI) m/z calculated for $C_{21}H_{22}ClN_2O_3S$ ($[M+H]^+$) 417.1040, found: 417.1020. Anal. $C_{21}H_{21}ClN_2O_3S$ (C, H, N).

*4.1.3.10. 11-[2-(Diethylamino)ethyl]-7-chloro-2,3-dimethoxybenzothiopyrano[3,2-b]indol-10(11H)-one (**5j**).* Yield, 30 %; m. p. 134-136 °C; ^{1}H NMR (400 MHz, $CDCl_3$): 1.52 (t, *J* = 7.2 Hz, 6H), 3.25 (q, *J* = 7.2 Hz, 4H), 3.46 (t, *J* = 7.4 Hz, 2H), 3.99 (s, 3H), 4.02 (s, 3H), 5.41 (t, *J* = 7.6 Hz, 2H), 7.05 (s, 1H), 7.48 (dd, J_{min} = 2.0 Hz, J_{max} = 8.8 Hz, 1H), 7.72 (d, *J* = 2.0 Hz, 1H), 7.89 (s, 1H), 8.59 (d, *J* = 8.8 Hz, 1H) ppm; ^{13}C-NMR (100 MHz, $CDCl_3$): δ 8.42 (2C), 40.85 (2C), 51.44, 56.59 (2C), 58.20, 94.28, 100.04, 115.14, 119,04, 125.94, 126.23, 126.99, 130.21, 131.04, 135.75, 137.29, 137.45, 147.17, 153.84, 171.39 ppm; HRMS (ESI) m/z calculated for $C_{23}H_{26}ClN_2O_3S$ ($[M+H]^+$) 445.1353, found: 445.1334. Anal. $C_{23}H_{25}ClN_2O_3S$ (C, H, N).

*4.1.3.11. 11-[2-(Dimethylamino)ethyl]-2,3,7-trimethoxybenzothiopyrano[3,2-b]indol-10(11H)-one (**5k**).* Yield, 50 %; m. p. 143-145 °C; ^{1}H NMR (400 MHz, $CDCl_3$): δ 2.47 (s, 6H), 2.87 (t, *J* = 7.4 Hz, 2H), 3.92 (s, 3H), 3.98 (s, 3H), 4.03 (s, 3H), 4.99 (t, *J* = 7.6 Hz, 2H), 7.02-7.07 (m, 4H), 8.60 (d, *J* = 8.4 Hz, 1H) ppm; ^{13}C-NMR (100 MHz, $CDCl_3$): δ 43.74, 45.69 (2C), 55.86, 56.56, 56.68, 59.25, 92.77, 100.49, 108.95, 114.87, 115.44, 118.44, 126.45 (2C), 130.72, 135.12, 137.90, 146.29, 152.19, 161.31, 172.02 ppm; HRMS (ESI) m/z calculated for $C_{22}H_{25}N_2O_4S$ ($[M+H]^+$) 413.1535, found: 413.1519. Anal. $C_{22}H_{24}N_2O_4S$ (C, H, N).

*4.1.3.12. 11-[2-(Diethylamino)ethyl]-2,3,7-trimethoxybenzothiopyrano[3,2-b]indol-10(11H)-one (**5l**).* Yield, 50 %; m. p. 151-153 °C; ^{1}H NMR (400 MHz, $CDCl_3$): δ 1.19 (t, *J* = 6.6 Hz, 6H), 2.83-2.85 (m, 4H), 3.05 (t, *J* = 7.4 Hz, 2H), 3.91 (s, 3H), 3.97 (s, 3H), 4.05 (s, 3H), 5.05 (t, *J* = 7.4 Hz, 2H), 7.03-7.06 (m, 3H), 7.21 (s, 1H), 8.58 (d, *J* = 9.2 Hz, 1H); ^{13}C-NMR (100 MHz, $CDCl_3$): δ 11.71 (2C), 47.56 (2C), 52.95, 55.97, 56.63 (2C), 57.02, 93.34, 100.42, 109.02, 115.01, 115.43, 118.36 126.44, 126.46, 130.75, 135.35, 138.04, 146.43, 152.39, 161.41, 172.07 ppm; HRMS (ESI): m/z calculated for $C_{24}H_{29}N_2O_4S$ ($[M+H]^+$) 441.1848, found: 441.1819. Anal. $C_{24}H_{28}N_2O_4S$ (C, H, N).

*4.1.3.13. 6-[2-(Dimethylamino)ethyl]-pyrido[3',2':5,6]thiopyrano[3,2-b]indol-5(6H)-one (**5m**).* Yield, 65 %; m. p. 138-140 °C; ^{1}H NMR (400 MHz, $CDCl_3$): δ 2.52 (s, 6H), 2.92 (t, *J* = 6.8 Hz, 2H), 5.11 (t, *J* = 6.8 Hz, 2H), 7.31 (t, *J* = 7.6 Hz, 1H), 7.48-7.52 (m, 1H), 7.60 (t, *J* = 7.6 Hz, 1H), 7.69-7.71 (m, 1H), 7.90 (d, *J* = 8.0 Hz, 1H), 8.82 (dd, J_{min} = 2.0 Hz, J_{max} = 8.4 Hz, 1H), 8.96 (dd, J_{min} = 2.0 Hz, J_{max} = 8.4 Hz, 1H) ppm; ^{13}C-NMR (100 MHz, $CDCl_3$): δ 22.84, 29.51, 29.85, 32.08, 111.24, 119.47, 121.16, 121.25, 121.37, 123.17, 127.38, 129.08, 129.26, 137.15, 139.86, 152.10, 157.90, 173.09 ppm; HRMS (ESI): m/z calculated for $C_{18}H_{18}N_3OS$ ($[M+H]^+$) 324.1171, found: 324.1153. Anal. $C_{18}H_{17}N_3OS$ (C, H, N).

*4.1.3.14. 6-[2-(Diethylamino)ethyl]-pyrido[3',2':5,6]thiopyrano[3,2-b]indol-5(6H)-one (**5n**).* Yield, 70 %; m. p. 101-103 °C; ^{1}H NMR (400 MHz, $CDCl_3$): δ 1.11 (t, *J* = 7.2 Hz, 6H), 2.75 (q, *J* = 7.2 Hz, 4H); 2.96 (t, *J* = 7.6 Hz, 2H), 5.03 (t, *J* = 7.6 Hz, 2H), 7.28 (t, *J* = 7.6 Hz, 1H), 7.47 (dd, J_{min} = 4.4 Hz, J_{max} = 8.4 Hz, 1H), 7.57 (t, *J* = 7.4 Hz, 1H), 7.68 (d, *J* = 8.8 Hz, 1H), 7.87 (d, *J* = 8.4 Hz, 1H), 8.79 (dd, J_{min} = 2.0 Hz, J_{max} = 4.4 Hz, 1H), 8.95 (dd, J_{min} = 1.8, Hz, J_{max} = 8.4 Hz, 1H) ppm; ^{13}C-NMR (100 MHz, $CDCl_3$): δ 11.82 (2C), 47.64 (2C), 53.14, 58.91, 111.23, 119.75, 121.02, 121.06, 121.11, 123.09, 127.51, 128.60, 129.29, 137.21, 139.93, 151.93, 157.79, 172.98 ppm; HRMS (ESI) m/z calculated for $C_{20}H_{22}N_3OS$ ($[M+H]^+$) 352.1484, found: 352.1465. Anal. $C_{20}H_{21}N_3OS$ (C, H, N).

*4.1.3.15. 6-[2-(Dimethylamino)ethyl]-9-methoxypyrido[3',2':5,6]thiopyrano[3,2-b]indol-5(6H)-one (**5o**).* Yield, 20 %; m. p. 104-106 °C. ^{1}H NMR (400 MHz, $CDCl_3$): δ 2.55 (s, 6H), 2.97 (t, *J* = 7.4 Hz, 2H), 3.92 (s, 3H), 5.08 (t, *J* = 7.6 Hz, 2H), 7.16 (d, *J* = 2.4 Hz, 1H), 7.24 (dd, J_{min} = 2.4 Hz, J_{max} = 9.2 Hz, 1H), 7.47 (dd, J_{min} = 4.4 Hz, J_{max} = 8.0 Hz, 1H), 7.63 (d, *J* = 9.2 Hz, 1H), 8.80 (dd, J_{min} = 2.2 Hz, J_{max} = 4.6 Hz, 1H), 8.92 (dd, J_{min} = 1.8 Hz, J_{max} = 8.0 Hz, 1H) ppm; ^{13}C-NMR (100 MHz, $CDCl_3$): δ 43.29, 45.31 (2C), 56.05, 59.83, 100.69, 112.31, 113.42, 120.86, 122.14, 122.47, 123.21, 126.73, 129.19, 135.25, 137.16, 152.00, 155.06, 172.91 ppm; HRMS (ESI) m/z calculated for $C_{19}H_{20}N_3O_2S$ ($[M+H]^+$) 354.1276, found: 354.1265. Anal. $C_{19}H_{19}N_3O_2S$ (C, H, N).

*4.1.3.16. 6-[2-(Diethylamino)ethyl]-9-methoxypyrido[3',2':5,6]thiopyrano[3,2-b]indol-5(6H)-one (**5p**).* Yield, 55 %; m, p. 98-100 °C; ^{1}H NMR (400 MHz, $CDCl_3$): δ 1.53 (t, *J* = 7.2 Hz, 6H), 3.28 (q, *J* = 7.2 Hz, 4H), 3.44 (t, *J* = 7.8, 2H), 3.92 (s, 3H), 5.45 (t, *J* = 7.6, 2H), 7.16 (d, *J* = 2.4 Hz, 1H), 7.34 (dd, J_{min} = 2.4 Hz, J_{max} = 9.2 Hz, 1H), 7.54 (dd, J_{min} = 4.8 Hz, J_{max} = 8.4 Hz, 1H), 8.16 (d, *J* = 9.2 Hz, 1H), 8.84 (dd, J_{min} = 1.6 Hz, J_{max} = 4.4 Hz, 1H), 8.95 (d, *J* = 8.0 Hz, 1H) ppm; ^{13}C-NMR (100 MHz, $CDCl_3$): δ 8.61 (2C), 46.93 (2C), 51.39, 56.25, 58.06, 100.82, 111.22, 113.38, 121.53, 122.06, 122.41, 123.41, 127.25, 129.25, 135.37, 137.59, 152.04, 155.76, 172.36 ppm; HRMS (ESI) m/z calculated for $C_{21}H_{24}N_3O_2S$ ($[M+H]^+$) 382.1589, found: 382.1575. Anal. $C_{21}H_{23}N_3O_2S$ (C, H, N).

*4.1.3.17. 6-[2-(Dimethylamino)ethyl]-9-chloropyrido[3',2':5,6]thiopyrano[3,2-b]indol-5(6H)-one (**5q**).* Yield, 25 %; m. p. 161-163 °C; ^{1}H NMR (400 MHz, $CDCl_3$): δ 2.38 (s, 6H), 2.76 (t, *J* = 7.0 Hz, 2H), 4.97 (t, *J* = 7.0 Hz, 2H), 7.49-7.54 (m, 3H), 7.84 (s, 1H), 8.81 (s, 1H), 8.94 (d, *J* = 8.0 Hz, 1H) ppm; ^{13}C-NMR (100 MHz, $CDCl_3$): δ 44.03, 45.98 (2C), 59.54, 112.30, 119.33, 120.34, 121.29, 123.84, 126.71, 128.21, 128.99, 129.23, 137.31, 138.17, 152.19, 157.66, 173.11 ppm; HRMS (ESI) m/z calculated for $C_{18}H_{17}ClN_3OS$ ($[M+H]^+$) 358.0781, found: 358.0766. Anal $C_{18}H_{16}ClN_3OS$ (C, H, N).

4.1.3.18. 6-*[2-(Diethylamino)ethyl]-9-chloropyrido[3',2':5,6]thiopyrano[3,2-b]indol-5(6H)-one (**5r**).* Yield, 35 %; m.p. 123-125 °C; ^{1}H NMR (400 MHz, $CDCl_3$): δ 1.02 (t, *J* = 7.0 Hz, 6H), 2.67 (q, *J* = 7.0 Hz, 4H), 2.88 (t, *J* = 7.2 Hz, 2H), 4.94 (t, *J* = 7.4 Hz, 2H), 7.46-7.49 (m, 2H), 7.57(d, *J* = 8.2 Hz, 1H), 7.82 (d, *J* = 1.6 Hz, 1H), 8.80 (dd, J_{min} = 1.8 Hz, J_{max} = 4.6 Hz, 1H), 8.93 (dd, J_{min} = 1.8 Hz, J_{max} = 8.2 Hz, 1H) ppm; ^{13}C-NMR (100 MHz, $CDCl_3$):δ 11.83 (2C), 47.6 (2C), 53.30, 58,91, 112.60, 119.87, 120.22, 121.25, 123.76, 126.58, 128.16, 128.89, 129.21, 137.29, 138.31, 152.15, 157.67, 173.09 ppm; HRMS (ESI) m/z calculated for $C_{20}H_{21}ClN_3OS$ ($[M+H]^+$) 386.1094, found: 386.1075. Anal. $C_{20}H_{20}ClN_3OS$ (C, H, N).

*4.1.3.19. 6-[2-(Dimethylamino)ethyl]-8,9-dimethoxypyrido[3',2':5,6]thiopyrano[3,2-b]indol-5(6H)-one (**5s**).* Yield, 20 %; m. p. 135-137 °C; ^{1}H NMR (400 MHz, $CDCl_3$): δ 2.93 (s, 6H), 3.56 (t, *J* = 7.4 Hz, 2H), 4.01 (s, 3H), 4.21 (s, 3H), 5.42 (t, *J* = 7.4 Hz, 2H), 7.13 (s, 1H), 7.50-7.53 (m, 1H), 7.82 (s, 1H), 8.83 (dd, J_{min} = 2.4 Hz, J_{max} = 8.4 Hz, 1H), 8.90 (dd, J_{min} = 1.8 Hz, J_{max} = 8.4 Hz, 1H) ppm; ^{13}C-NMR (100 MHz, $CDCl_3$): δ 41.04, 43.45 (2C), 56.57, 57.36, 57.97, 93.70, 100.22, 115.61, 121.36, 124.78, 125.63, 128.85, 136.19, 137.05, 147.27, 151.66, 153.99, 157.42, 173.18 ppm; HRMS (ESI) m/z calculated for $C_{20}H_{22}N_3O_3S$ ($[M+H]^+$) 384.1382, found: 384.1354. Anal. $C_{20}H_{21}N_3O_3S$ (C, H, N).

*4.1.3.20. 6-[2-(Diethylamino)ethyl]-8,9-dimethoxypyrido[3',2':5,6]thiopyrano[3,2-b]indol-5(6H)-one (**5t**).* Yield, 25 %; m. p. 142-144 °C; ^{1}H NMR (400 MHz, $CDCl_3$): δ 1.52 (t, *J* = 7.2 Hz, 6H), 3.22-3.29 (m, 4H), 3.45 (t, *J* = 7.2 Hz, 2H), 3.97 (s, 3H), 4.20 (s, 3H), 5.40 (t, *J* = 7.6 Hz, 2H), 7.05 (s, 1H), 7.48 (dd, J_{min} = 4.4 Hz, J_{max} = 8.4 Hz, 1H), 7.87 (s, 1H), 8.79 (dd, J_{min} = 1.8 Hz, J_{max} = 8.6 Hz, 1H), 8.88 (dd, J_{min} = 1.8 Hz, J_{max} = 8.2 Hz, 1H) ppm; ^{13}C-NMR (100 MHz, $CDCl_3$): δ 8.27 (2C), 40.63 (2C), 46.38, 51.26, 56.46, 58.07, 93.98, 99.98, 115.35, 121.22, 125.76 (2C), 128.92, 136.10, 136.87, 147.07, 151.62, 153.90, 157.48, 171.43 ppm; HRMS (ESI) m/z calculated for $C_{22}H_{26}N_3O_3S$ ($[M+H]^+$) 412.1695, found: 412.1690. Anal. $C_{22}H_{25}N_3O_3S$ (C, H, N).

4.2 Biological evaluation

4.2.1 Cell Cultures

HeLa (human cervix adenocarcinoma cells) were grown in Nutrient Mixture F-12 [HAM] (Sigma Chemical Co.), MSTO-211H (human biphasic mesothelioma cells) and MeT-5A (human mesothelium cells) were grown in RPMI (Sigma Chemical Co.) supplemented with 2.38 g/L Hepes, 0.11 g/L pyruvate sodium and 2.5 g/L glucose, A431 (human squamous carcinoma cells) were grown in Dulbecco's Modified Eagle's Medium (Sigma Chemical Co.). 10% Heat-inactivated fetal calf serum (Invitrogen), 100 U/mL penicillin, 100 μg/mL streptomycin and 0.25 μg/mL amphotericin B

(Sigma Chemical Co.) were added to the media. The cells were cultured at 37 °C in a moist atmosphere of 5% carbon dioxide in air.

4.2.2 Inhibition Growth Assay

Cells ($3\text{-}4\times10^4$) were seeded into each well of a 24-well cell culture plate. After incubation for 24 h various concentrations of the test agents were added and the cells were then incubated in standard conditions for a further 72 h. A trypan blue assay was performed to determine cell viability. Cytotoxicity data were expressed as GI_{50} values, i.e. the concentration of the test agent inducing 50% reduction in cell number compared with control cultures.

4.2.3 Evaluation of apoptotic cell death by Annexin V-FITC and propidium iodide staining.

To detect cellular apoptosis, a FITC Annexin V Apoptosis Detection Kit I (BD Pharmigen) was used. HeLa cells (5×10^5) were seeded into each cell culture plate in complete growth medium. After incubation for 24 h the test agent was added at the indicated concentrations and cells were incubated for a further 18 h. After treatment, cells were centrifuged and resuspended at 10^6 cells/mL in binding buffer. Cell suspensions (100 μL) were added with Annexin V-FITC and propidium iodide (PI) as indicated by the supplier's instructions, and incubated for 15 min at room temperature in the dark. The populations of Annexin V-negative/PI-negative (viable), Annexin V-positive/PI-negative (early apoptosis), Annexin V-positive/PI-positive (late apoptosis) and Annexin V-negative/PI-positive (necrosis) cells were evaluated by FACSCanto II flow cytometer (Becton–Dickinson, Mountain View, CA).

4.2.4 Linear Flow Dichroism

Linear dichroism (LD) measurements were performed on a Jasco J500A circular dichroism spectropolarimeter, converted for LD and equipped with an IBM PC and a Jasco J interface.

Linear dichroism was defined as:

$$LD_{(\lambda)} = A_{//(\lambda)} - A_{\perp(\lambda)}$$

where $A_{//}$ and $A_{\perp}$ correspond to the absorbances of the sample when polarized light was oriented parallel or perpendicular to the flow direction, respectively. The orientation was produced by a device

designed by Wada and Kozawa [41] at a shear gradient of 500-700 rpm, and each spectrum was accumulated twice.

Aqueous solutions of salmon testes DNA (1.9 x 10^{-3}M) in 10 mM TRIS, 1 mM EDTA (pH 7.0) and 0.01 M NaCl were used. Spectra were recorded at 25 °C at [drug]/[DNA]=0, 0.02 and 0.04.

4.2.5 Topoisomerase-Mediated DNA Relaxation.

Supercoiled pBR322 plasmid DNA (0.25 μg, Fermentas Life Sciences) was incubated with 1U Topo II (human recombinant Topo II α, USB Corporation) or 2U Topo I (human recombinant Topo I, TopoGen) and the test compounds as indicated, for 60 min at 37 °C in 20 μL reaction buffer.

Reactions were stopped by adding 4 μL stop buffer (5% sodium dodecyl sulfate (SDS), 0.125% bromophenol blue, and 25% glycerol), 50 μg/mL proteinase K (Sigma) and incubating for a further 30 min at 37 °C. The samples were separated by electrophoresis on 1% agarose gel at room temperature. The gels were stained with ethidium bromide 1 μg/mL in TAE buffer (0.04 M Tris-acetate and 0.001 M EDTA), transilluminated by UV light, and fluorescence emission was visualized by a CCD camera coupled to a Bio-Rad Gel Doc XR apparatus.

4.2.6 Topoisomerase-mediated DNA cleavage.

10 U Topo II (human recombinant Topo II α, USB) or 5 U Topo I (human recombinant topoisomerase I, TopoGen) were incubated with supercoiled pBR322 plasmid DNA, 0.25 μg or 20 ng, respectively and the test compounds, as indicated, for 60 min at 37 °C in 20 μL reaction buffer.

Reactions were stopped by adding 4 μL stop buffer (5% SDS, 0.125% bromophenol blue and 25% glycerol), 50 μg/mL proteinase K (Sigma) and incubating for a further 30 min at 37 °C. The samples were separated by electrophoresis on 1% agarose gel containing ethidium bromide 0.5 μg/mL in TBE buffer (0.09 M Tris-borate and 0.002 M EDTA), transilluminated by UV light, and fluorescence emission was visualized by a CCD camera coupled to a Bio-Rad Gel Doc XR apparatus.

4.3 Molecular Modeling.

As for the protein structure selection, we chose the highest resolution (2.10 Å) crystal structure of the human Topo I in complex with the poison **2** and covalent complex with a 22 bp DNA duplex (PDB code: 1K4T). The other ternary complex available in the PDB databank diffract to such a limited resolution (3.0 Å or above), that did not allow for the placement of water molecules.

4.3.1 Hydrated docking.

The new version of the docking program AutoDock (version 4.2, AD4) [34], as implemented through the graphical user interface called AutoDockTools (ADT), was used to perform docking studies. The ligand structures were built using the builder in the Maestro package of Schrödinger Suite and optimized using MacroModel (version 9.9) [42]. The constructed compounds were converted into AD4 format files using ADT and hydrated using the wet.py python script. Protein structure (PDB code: 1K4T) was prepared using the Protein Preparation Wizard through the graphical user interface of Maestro 9.3 [43]. Water molecules were removed and hydrogen atoms were added and minimized using the all-atom OPLS-2005 force field. The receptor was also converted in the AD4 format file using ADT. Gasteiger-Marsili partial charges were then assigned to the ligands and the receptor. The docking area was centered around the ligand binding site. A set of grids of 85 × 85 × 85 with 0.375 Å spacing was calculated around the docking area for the ligand atom types using AutoGrid 4.2. An additional grid map was calculated for the water molecules using the mapwater.py suite. For each ligand, 100 separate docking calculations were performed. Each docking calculation consisted of 10 million energy evaluations using the Lamarckian genetic algorithm local search (GALS) method. The GALS method evaluates a population of possible docking solutions and propagates the most successful individuals from each generation into the subsequent generation of possible solutions. A low-frequency local search according to the method of Solis and Wets is applied to docking trials to ensure that the final solution represents a local minimum. All dockings described in this paper were performed with a population size of 250, and 300 rounds of Solis and Wets local search were applied with a probability of 0.06. A mutation rate of 0.02 and a crossover rate of 0.8 were used to generate new docking trials for subsequent generations, and the best individual from each generation was

propagated over the next generation. The docking results from each of the 100 calculations were clustered on the basis of root-mean square deviation (RMSD) (solutions differing by <2.0 Å) between the Cartesian coordinates of the atoms and were ranked on the basis of free energy of binding (ΔG_{AD4}). To refine the AD4 output, the complexes found were energy minimized through a molecular mechanics/energy minimization (MM/EM) approach. The computational protocol applied consisted of the application of 15000 steps of the Polak–Ribiére conjugate gradients (PRCG) or until the derivative convergence was 0.05 kJ/mol. Pictures were rendered using Pymol (https://pymol.org/2/) and Chimera software package [44].

AUTHOR INFORMATION

Corresponding Authors

* To whom all correspondence should be addressed. S. Taliani, Tel: ++39 0502219547; E-mail: sabrina.taliani@unipi.it. L. Marinelli, Tel: ++39 081679899; E-mail: lmarinel@unina.it.

Author Contributions

The manuscript was written through contributions of all authors. All authors have given approval to the final version of the manuscript. ‡ These authors contributed equally.

Funding: This work was supported by the University of Pisa (PRA Project, PRA_2018_20).

Appendix A. Supplementary data.

Supplementary data related to this article for publication on line.

References

[1] A. Rescifina, C. Zagni, M.G. Varrica, V. Pistara, A. Corsaro, Recent advances in small organic molecules as DNA intercalating agents: synthesis, activity, and modeling. Eur. J. Med. Chem. 74 (2014) 95-115.

[2] A. Jemal, F. Bray, M.M. Center, J. Ferlay, E. Ward, D. Forman, Global cancer statistics. CA-Cancer J. Clin. 61 (2011) 69-90.

[3] D.J. Newman, G.M. Cragg, K.M. Snader, Natural products as sources of new drugs over the period 1981–2002. J. Nat. Prod. 66 (2003) 1022–1037.

[4] A. Ali, S. Bhattacharya, DNA binders in clinical trials and chemotherapy. Bioorg. Med. Chem. 22 (2014) 4506-4521.

[5] M.F. Brana, M. Cacho, A. Gradillas, B. de Pascual-Teresa, A. Ramos, Intercalators as anticancer drugs. Curr. Pharm. Des. 7 (2001) 1745–1780.

[6] C. Bailly, Contemporary challenges in the design of topoisomerase II inhibitors for cancer chemotherapy. Chem. Rev. 112 (2012) 3611−3640.

[7] J.L. Nitiss, Targeting DNA topoisomerase II in cancer chemotherapy. Nat. Rev. Cancer 9 (2009) 338−350.

[8] J.C. Wang, DNA topoisomerases. Annu. Rev. Biochem. 65 (1996) 635-692.

[9] J.L. Nitiss, Investigating the biological function of DNA topoisomerases in eukaryotic cells. Biochim. Biophys. Acta, Gene Struct. Expression 1400 (1998) 63−81.

[10] S.M. Vos, E.M. Tretter, B.H. Schmidt, J.M. Berger, All tangled up: how cells direct, manage and exploit topoisomerase function. Nat. Rev. Mol. Cell Biol. 12 (2011) 827−841.

[11] L. Stewart, M.R. Redimbo, X. Qiu, W.G.J. Hol, J.J. Champoux, A model for the mechanism of human topoisomerase I. Science 279 (1998) 1534-1541.

[12] G. Capranico, J. Marinello, G. Chillemi, Type I DNA topoisomerases. J. Med. Chem. 60 (2017) 2169-2192.

[13] J.M. Berger, S.J. Gamblin, S.C. Harrison, J.C. Wang, Structure and mechanism of DNA topoisomerase II. Nature 379 (1996) 225-232.

[14] J.L. Nittis, DNA topoisomerase II and its growing repertoire of biological functions. Nat. Rev. Cancer 9 (2009) 327-337.

[15] Y. Pommier, Y. Sun, S.N. Huang, J.L. Nitiss, Roles of eukaryotic topoisomerases in transcription, replication and genomic stability. Nat. Rev. Mol. Cell Biol. 17 (2016) 703-721.

[16] S.M. Cuya, M.A. Bjornsti, R. van Waardenburg, DNA topoisomerase-targeting chemotherapeutics: what's new? Cancer Chemother. Pharmacol. 80 (2017) 1-14.

[17] S. Salerno, F. Da Settimo, S. Taliani, F. Simorini, C. La Motta, G. Fornaciari A.M. Marini, Recent advances in the development of dual topoisomerase I and II Inhibitors as anticancer drugs. Curr. Med. Chem. 17 (2010) 4270-4290.

[18] Y. Pommier, E. Leo, H. Zhang, C. Marchand, DNA topoisomerases and their poisoning by anticancer and antibacterial drugs. Chem. Biol. 17 (2010) 421-433.

[19] Y. Pommier, Topoisomerase I inhibitors: camptothecins and beyond. Nat. Rev. Cancer 6 (2006) 789-802.

[20] G. Hu, D. Zekria, X. Cai, X. Ni, Current status of CPT and its analogues in the treatment of malignancies. Phytochem. Rev. 14 (2015) 429-441.

[21] Y. Pommier, DNA topoisomerase I inhibitors: chemistry, biology, and interfacial inhibition. Chem. Rev. 109 (2009) 2894−2902.

[22] Y. Xu, C. Her, Inhibition of topoisomerase (DNA) I (TOP1): DNA damage repair and anticancer therapy. Biomolecules 5 (2015) 1652-1670.

[23] Y. Pommier, Drugging topoisomerases: lessons and challenges. ACS Chem. Biol. 8 (2013) 82−95.

[24] M.E. Wall, M.C. Wani, C.E. Cook, K.H. Palmer, A.T. McPhail, G. A. Sim, Plant antitumor agents. I. The isolation and structure of campthotecin, a novel alkaloidal leukemia and tumor inhibitor from Camptotheca acuminata. J. Am. Chem. Soc. 88 (1966) 3888-3890.

[25] Z.A. Rasheed, E.H. Rubin, Mechanisms of resistance to topoisomerase I-targeting drugs. Oncogene 22 (2003) 7296-7304.

[26] A. Da Settimo, F. Da Settimo, A.M. Marini, G. Primofiore, S. Salerno, G. Viola, L. Dalla Via, S. Marciani Magno, Synthesis, DNA binding and in vitro antiproliferative activity of purinoquinazoline, pyridopyrimidopurine and pyridopyrimidobenzimidazole derivatives as potential antitumor agents. Eur. J. Med. Chem. 33 (1998) 685–696.

[27] A. Da Settimo, A.M. Marini, G. Primofiore, F. Da Settimo, S. Salerno, F. Simorini, G. Pardi, C. La Motta, D. Bertini, Synthesis of novel 1,4-dihydropyrido[3′,2′:5,6]thiopyrano[4,3-*c*]pyrazoles and 5*H*-pyrido[3′,2′:5,6]thiopyrano[4,3-*d*]pyrimidines as potential antiproliferative agents J. Heterocycl. Chem. 39 (2002) 1001-1006.

[28] L. Dalla Via, O. Gia, S. Marciani Magno, A. Da Settimo, G. Primofiore, F. Simorini, A.M. Marini, F. Da Settimo, Dialkylaminoalkylindolonaphthyridines as potential antitumour agents: synthesis, cytotoxicity and DNA binding properties. Eur. J. Med. Chem. 37 (2002) 475–486.

[29] S. Taliani, I. Pugliesi, E. Barresi, S. Salerno, C. Marchand, K. Agama, F. Simorini, C. La Motta, A.M. Marini, F.S. Di Leva, L. Marinelli, S. Cosconati, E. Novellino, Y. Pommier, R. Di Santo, F. Da Settimo, Phenylpyrazolo[1,5-*a*]quinazolin-5(4H)-one: a suitable scaffold for the development of noncamptothecin topoisomerase I (Top1) inhibitors. J. Med. Chem. 56 (2013) 7458-7462.

[30] L. Dalla Via, S. Marciani Magno, O. Gia, A.M. Marini, F. Da Settimo, S. Salerno, C. La Motta, F. Simorini, S. Taliani, A. Lavecchia, C. Di Giovanni, G. Brancato, V. Barone, E. Novellino, Benzothiopyranoindole-based antiproliferative agents: synthesis, cytotoxicity, nucleic acids interaction, and topoisomerases inhibition properties. J. Med. Chem. 52 (2009) 5429–5441.

[31] T. Moriwake, Synthesis of 3-cyano-3-methyl-4-thiochromanone and 3-carbomethoxy-3-methyl-4-thiochromanone. J. Med. Chem. 9 (1966) 163-164.

[32] R.R. Phillips, The Japp-Klingemann reaction. Org. Reactions 10 (1959) 143-178.

[33] B.L. Staker, K. Hjerrild, M.D. Feese, C.A. Behnke, A.B. Burgin, L. Stewart, The mechanism of topoisomerase I poisoning by a camptothecin analog. Proc. Natl. Acad. Sci. U. S. A. 99 (2002) 15387-15392.

[34] R. Huey, G.M. Morris, A.J. Olson, D.S. Goodsell, A semiempirical free energy force field with charge-based desolvation. J. Comput. Chem. 28 (2007) 1145-1152.

[35] S. Forli, A.J. Olson, A force field with discrete displaceable waters and desolvation entropy for hydrated ligand docking. J. Med. Chem. 55 (2012) 623-638.

[36] Y. Pommier, P. Pourquier, Y. Urasaki, J. Wu, G.S. Laco, Topoisomerase I inhibitors: selectivity and cellular resistance. Drug Resist. Updat. 2 (1999) 307-318.

[37] B.L. Staker, M.D. Feese, M. Cushman, Y. Pommier, D. Zembower, L. Stewart, A.B. Burgin, Structures of three classes of anticancer agents bound to the human topoisomerase I-DNA covalent complex. J. Med. Chem. 48 (2005) 2336-2345.

[38] S. Antony, M. Jayaraman, G. Laco, G. Kohlhagen, K.W. Kohn, M. Cushman, Y. Pommier, Differential induction of topoisomerase I-DNA cleavage complexes by the indenoisoquinoline MJ-III-65 (NSC 706744) and camptothecin: base sequence analysis and activity against camptothecin-resistant topoisomerases I. Cancer Res. 63 (2003) 7428-7435.

[39] Y. Urasaki, G. Laco, Y. Takebayashi, C. Bailly, G. Kohlhagen, Y. Pommier, Use of camptothecin-resistant mammalian cell lines to evaluate the role of topoisomerase I in the antiproliferative activity of the indolocarbazole, NB-506, and its topoisomerase I binding site. Cancer Res. 61 (2001) 504-508.

[40] A. Ioanoviciu, S. Antony, Y. Pommier, B.L. Staker, L. Stewart, M. Cushman, Synthesis and mechanism of action studies of a series of norindenoisoquinoline topoisomerase I poisons reveal an inhibitor with a flipped orientation in the ternary DNA-enzyme-inhibitor complex as determined by X-ray crystallographic analysis. J. Med. Chem. 48 (2005) 4803-4814.

[41] A. Wada, S. Kozawa, Instrument for the studies of differential flow dichroism of polymer solutions. J. Polym. Sci., Part A: Gen. Pap. 2 (1964) 853-864.

[42] MacroModel, v., Schrödinger, LLC, New York, NY, 2012.

[43] Maestro, v., Schrödinger, LLC, New York, NY, 2012.

[44] E.F. Pettersen, T.D. Goddard, C.C. Huang, G.S. Couch, D.M. Greenblatt, E.C. Meng, T.E. Ferrin, UCSF Chimera - a visualization system for exploratory research and analysis. J. Comput. Chem. 25 (2004) 1605-1612.